Photophysics and Ultrafast Relaxation Dynamics of the Excited States of Dimethylaminobenzophenone

Ajay K. Singh, G. Ramakrishna, Hirendra N. Ghosh, and Dipak. K. Palit*

Radiation Chemistry & Chemical Dynamics Division, Bhabha Atomic Research Centre, Mumbai 400 085, India

Received: October 16, 2003; In Final Form: February 10, 2004

Steady-state as well as time-resolved absorption and emission studies in the femto-, pico-, and nanosecond time-domains have been performed to investigate the relaxation dynamics and the photophysical properties of dimethylaminobenzophenone (DMABP) by characterizing its excited singlet (S_1) and triplet (T_1) state properties in different kinds of solvents. Large bathochromic shifts of the steady-state absorption maximum in more polar solvents suggest an intramolecular charge transfer (ICT) character of the S_1 state. DMABP is weakly fluorescent but shows the features of "dual-fluorescence". Dynamics of very efficient nonradiative relaxation process in the S_1 state of DMABP has been described by invoking a "three state model", in which the involvement of the ground state and two adiabatically coupled S_1 states, a locally excited (LE) $\pi\pi^*$ or ICT state and a conformationally relaxed or twisted intramolecular charge transfer (TICT) state, have been considered. In aprotic solvents, the fluorescence maximum arises due to emission from the TICT state. On the other hand, in alcohols, the fluorescence maximum arises due to emission from the LE state, since the TICT state is weakly fluorescent due to strong intermolecular hydrogen-bonding interaction with the solvent. The excited-state relaxation process follows multiexponential dynamics. An ultrafast component, having lifetime τ_1, which varies in the range 0.2−0.5 ps in different polar solvents, may possibly originate from either the relaxation of the solvent-perturbed low-frequency intramolecular modes or the inertial solvation of the ICT state. The lifetime of another slower component ($\tau_2 \sim 0.2-5$ ps) increases linearly with an increase in the viscosity of the solvent. This component has been attributed to the diffusive twisting motion of the dimethylaminophenyl group with respect to the benzoyl group. This twisting process with a rate, which is comparable to or faster than the average solvation time of the solvent, is associated with the crossing of a low barrier (or quasi-barrierless) and responsible for the population relaxation in the S_1 state. The third component ($\tau_3 \sim 5-900$ ps), which is sensitive to the hydrogen bonding ability of the solvent, represents the decay of the S_1 state to the ground state. The spectroscopic nature, energy, and yield of the T_1 state are very sensitive to the characteristics of the solvent or medium.

1. Introduction

For several decades, steady-state and time-resolved phosphorescence spectroscopy as well as flash photolysis techniques have been used to study the photophysical and photochemical properties of the excited singlet and triplet states of benzophenone and its numerous kinds of derivatives by different groups.[1−15] Most of these studies have been devoted to unraveling the intricacies of the mechanisms of photoreduction reactions undergone by the aromatic carbonyl compounds in the presence of hydrogen atom donors. The rate and efficiency of this process have been shown to depend on the nature of the hydrogen atom donor as well as the nature of the substituents on the aromatic rings.[7,10,11,16−20] The substituents on the aromatic rings influence the relative positions of two kinds of electronic excited states, namely, $n\pi^*$ and $\pi\pi^*$ states, on the energy scale in both the singlet as well as the triplet manifolds.[21−23] Both the lowest excited singlet (S_1) and triplet (T_1) states of benzophenone have $n\pi^*$ character in all kinds of solvents.[24−26] However, on introduction of the electron donating groups, such as OH, NH_2, $N(CH_3)_2$, OCH_3, etc, onto the aromatic rings of benzophenone, the nature of the S_1 and T_1 states becomes dependent on solvent polarity.[22,26,27] The derivatives of benzophenone, which have the S_1 and T_1 states with $\pi\pi^*$ character, are characterized with longer lifetimes, lower triplet quantum yields, as well as reduced photochemical reactivities as compared to those of the $n\pi^*$ type states.[26−31]

Recently, we reported the results of our investigations on the properties of the excited singlet and triplet states of the hydroxy- and amino-substituted benzophenone derivatives using time-resolved fluorescence and absorption spectroscopic techniques [27,30,31] Whereas benzophenone and its hydroxy-substituted derivatives have been seen to be nearly nonfluorescent, the amino-substituted derivatives are weakly fluorescent.[30−33] We observed significantly large bathochromic shifts of both the absorption and fluorescence maxima of *p*-aminobenzophenone (PABP) and Michler's ketone (MK) in more polar solvents. This indicated a strong intramolecular charge-transfer (ICT) character of the S_1 state.[30,31] We also observed a large Stokes shift between the fluorescence and absorption maxima in all aprotic solvents. However, the laser flash photolysis equipment used for these studies had about 0.5 ps time resolution, and we could not reveal any other kind of relaxation dynamics, which was faster than the singlet−triplet intersystem-crossing process as well as other decay processes taking place from the S_1 state. Recently, we developed a femtosecond transient absorption spectrometer,

* To whom correspondence should be addressed. E-mail: dkpalit@apsara.barc.ernet.in. Tel: 91-22-25595091. Fax: 91-22-25505151/25519613.

10.1021/jp037132+ CCC: $27.50
Published on Web 03/12/2004

SCHEME 1: Chemical Structure of the DMABP Molecule

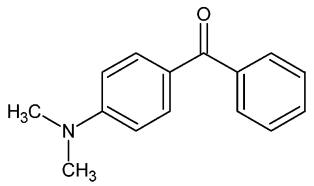

which has a time resolution of about 120 fs. This has helped us to study the early-time dynamics in the S_1 state of DMABP. We observe the conformational relaxation process via twisting of the dimethylaminophenyl group in the S_1 state of DMABP, prior to the intersystem-crossing process. This explains the reason for the large Stokes shift of the fluorescence emission maximum in amino-substituted benzophenones. Earlier, Prater et al. indicated the possibility of quasi-barrierless torsional motion of the phenyl group in 4-phenylbenzophenone.[34] Recently, Glasbeek and co-workers, who studied the relaxation dynamics of MK using fluorescence upconversion technique with about 150 fs time resolution, explained their results by invoking the concept of a potential energy surface (PES) consisting of two adiabatic states, which have twist angle dependent electronic wave functions.[32] One of these states is assigned to an un-relaxed emissive type locally excited (LE) state, and the other one is assigned to the geometrically relaxed nonemissive or weakly emissive charge-transfer (CT) state (see Scheme 1).

Conformational relaxation via molecular twisting has been one of the puzzling processes of the molecular photoreactions in the condensed phase. A coupling between charge transfer and conformational relaxation via twisting of the dimethylamino group was first suggested by Grabowski and co-workers in order to describe the dynamical relaxation process in the S_1 state of the *p*-*N*,*N*-dimethylaminobenzonitrile (DMABN) molecule.[35] The concept of LE and "twisted intramolecular charge transfer" (TICT) states were evoked to describe the dual fluorescence observed for this molecule. Since then, charge transfer and conformational relaxation processes in different classes of flexible donor−acceptor molecules with the dimethylaminophenyl group as the donor have been widely discussed in the literature.[35−47] Depending on the mechanism of the deactivation processes taking place in the S_1 state, either or both of these two states are fluorescent or nonfluorescent. Hence, "dual-fluorescence" may not be a common feature for all of the molecules showing TICT behavior. Based on the results reported so far on such kinds of molecular systems, the molecules could be classified into two distinct classes. In one class of molecules, the Franck−Condon (FC) state or the LE state has a dipole moment, which is very similar to that of the ground state and the CT process is initiated by photoexcitation and accompanied by solvation and conformational relaxation. Experiments with this class of molecules give evidence for the formation of the TICT state through a barrierless or quasi-barrierless process of twisting of the dimethylaminophenyl group in an ultrafast time-domain. The TICT state could be either a fluorescent state with a nonfluorescent LE state (for example, in the case of the merocyanine DCM dye) or a nonfluorescent state with a fluorescent LE state (for example, in the case of amino-rhodamine and di- and tri-phenyl methane dyes and auramine).[36−42] In the case of dimethylaminobenzonitrile, substituted triphenylphosphine derivatives and donor−acceptor type stilbene molecules, which show the properties of dual-fluorescence, both the LE and the TICT states are fluorescent.[34−45] In another class of molecules, the LE state is an ICT state and solvation and conformational changes are the two relaxation processes taking place simultaneously following photoexcitation. Amino-substituted fluorenones and triarylpyrylium cations constitute this class of molecules.[46,47] In both cases, the LE state is fluorescent but the conformationally relaxed TICT state is nonfluorescent. Recently, Gustavsson and co-workers, who reported the "charge-transfer induced twisting" dynamics in *N*,*N*-dimethylaminobenzylidene-3-indanone, suggested that the central C═C bond is responsible for the twisting process.[48] This bond is substantially weakened in the excited state as compared to that of the C−C single bond. In this case, the LE state is an ICT state, which is fluorescent, and the conformationally relaxed or twisted state is a "dark" (nonfluorescent) state. The present study shows that the amino-substituted benzophenones also can be classified with the molecules of the latter class, for which the LE state is an ICT state. However, our study on DMABP suggests different kinds of dynamical behaviors in different kinds of solvents and emission characteristics of the LE and TICT states depend on the characteristics of the solvent medium.

2. Experimental Section

DMABP (Aldrich, 98% pure) was used after recrystallization from aqueous ethanol. All of the solvents used were of spectroscopic grade (Spectro-Chem, India) and were used as received without further purification. Steady-state absorption spectra were recorded on a Shimadzu model UV-160A spectrophotometer. Fluorescence spectra were recorded using a Hitachi model 4010 spectrofluorimeter. The fluorescence yields, ϕ_F, were determined by comparing the areas under the fluorescence curves with that of a standard, *p*-aminobenzophenone (PABP) in benzene ($\phi_F = 1.2 \times 10^{-3}$), under the same experimental conditions.[30] No correction has been made for variation of refractive indices of the solvents. High-purity grade nitrogen gas (Indian Oxygen, purity >99.9%) was used to deaerate the samples.

Three different time-resolved techniques were used to study the dynamics of the excited state. The fluorescence lifetimes were measured using a time-correlated single photon counting spectrometer with 20 ps time resolution.[49] The transient absorption spectra were recorded with 35 ps time-resolution using a picosecond laser flash photolysis apparatus, the details of which have been described in refs 30 and 31. Briefly, the third harmonic output (355 nm, 5 mJ) from an active passive mode-locked Nd:YAG laser (Continuum, model 501-C-10) providing 35 ps pulses was used for excitation, and the continuum (400−950 nm) probe pulses were generated by focusing the residual fundamental in a 10 cm cell containing a H_2O/D_2O mixture. The probe pulses were delayed with respect to the pump pulses using an 1 m long linear translation stage and the transient absorption signal at different probe delays (up to 6 ns) were recorded with an optical multichannel analyzer (Spectroscopic Instruments, Germany) interfaced to an IBM-PC. The zero delay position was assigned to that when the probe light reached the sample just after the end of the pump pulse. The species surviving beyond 100 ns were studied using a nanosecond flash-photolysis setup, which uses the same picosecond Nd:YAG laser for excitation and a cw tungsten lamp, in combination with a Bausch & Lomb monochromator (350−800 nm), a Hamamatsu R-928 PMT, and a 500 MHz digital oscilloscope (Tektronix, TDS-540A) connected to a PC, to probe the transient absorption. Using the same set up, but without the probe light, phosphorescence lifetimes in rigid matrixes at 77 K were also determined.

Relaxation processes faster than 50 ps were measured using a femtosecond pump−probe spectrometer. The pulses of 6 nJ

TABLE 1: Photophysical Properties of DMABP

solvent	λ_{abs}(max), nm (cm^{-1})	λ_F(max), nm (ν_F, cm^{-1})	Stokes' shift (cm^{-1})	τ_F, ps	ϕ_F, 10^{-3}	ϕ_T	ϕ_{IC}	k_R,[a] 10^7 s^{-1}	K_{NR},[b] 10^9 s^{-1}	τ_T, μs	τ_{Ph}, ms
cyclohexane	325 (30769)	462 (21645)	9124	100	1.1	0.92	0.08	1.1	10.0	0.07	3.8, 48
benzene	340 (29412)	497 (20121)	9291	900	6.7	0.42	0.57	0.74	1.1	7.7	1, 66
acetonitrile	345 (28986)	602 (16612)	12 374	160	0.32	0.06	0.94	0.20	6.2	9	63
DMSO	350 (28571)	609 (16420)	12 151	100	0.34	0.05	0.95	0.38	10.0	10	
methanol	355 (28169)	480 (20833)	7336	5.2[c]	0.05		~100	4	200		90

[a] $k_R = \phi_F/\tau_F$. [b] $k_{NR} = (1-\phi_F)/\tau_F$. [c] Value from transient absorption data. Percentage of errors involved: 5% in τ_F and ϕ_T and 10% in ϕ_F.

energy at 800 nm were obtained from a self-mode-locked Ti: sapphire laser, which is pumped by a 5 W DPSS. These pulses were amplified to generate 50 fs laser pulses of about 250 μJ energy using chirped pulse amplification (CPA) technique. The amplifier consists of a pulse stretcher, a Nd:YAG laser pumped multipass amplifier, and a compressor. One part of the amplifier output was frequency doubled in a 0.5 mm BBO crystal to generate pump pulses at 400 nm for excitation of the samples and the other part was used to generate the white light continuum (470−1000 nm) in a 2 mm thin sapphire plate for probing the transient absorption induced by the pump. The sample solutions were kept flowing through a quartz cell of 1 mm path length. The polarization of the pump beam was kept at the magic angle, and the energy of this beam was maintained at ≤ 5 μJ. The decay dynamics at a particular wavelength region (10 nm width) were monitored using two photodiodes coupled with the boxcar integrators and the time-resolved transient absorption spectra were constructed from the temporal profiles recorded at different wavelengths. The overall time resolution of the absorption spectrometer was determined to be about 120 fs by measuring the growth of the $S_1 \rightarrow S_n$ absorption of perylene in acetonitrile solution at 690 nm. The temporal profiles were fitted with multiexponential functions by iterative de-convolution analysis using $Sech^2$ type instrument response function having 120 fs fwhm.

3. Results

3.1. Steady-State Studies. The ground-state absorption and emission spectra of DMABP have been recorded in several solvents with varying polarities and hydrogen bonding abilities. The absorption spectra in some typical solvents, namely, cyclohexane (nonpolar), benzene (nondipolar), acetonitrile and DMSO (polar but aprotic), and methanol (polar as well as protic), are presented in Figure 1A. The absorption spectrum in cyclohexane exhibits an intense absorption band with maximum at 325 nm (30769 cm^{-1}). With increase in solvent polarity, the maximum of the absorption band shows a large bathochromic shift. For example, the absorption maximum shifts by about 1783 and 2198 cm^{-1} in acetonitrile and DMSO, respectively, as compared to that in cyclohexane (Table 1). We also observe a small shoulder at ca. 310 nm (32 258 cm^{-1}) in polar solvents. In addition, the spectral width of the absorption band also increases marginally in more polar solvents.

Unlike the parent BP molecule, which is nearly nonfluorescent, DMABP is weakly fluorescent like other amino-substituted benzophenone derivatives, say, PABP and MK.[30−33] Figure 1B shows the fluorescence spectra of DMABP in various organic solvents. In each of the solvents, the fluorescence spectrum consists of a structureless broad band. The fluorescence maximum, λ_F(max) or ν_F, as well as the shape of the

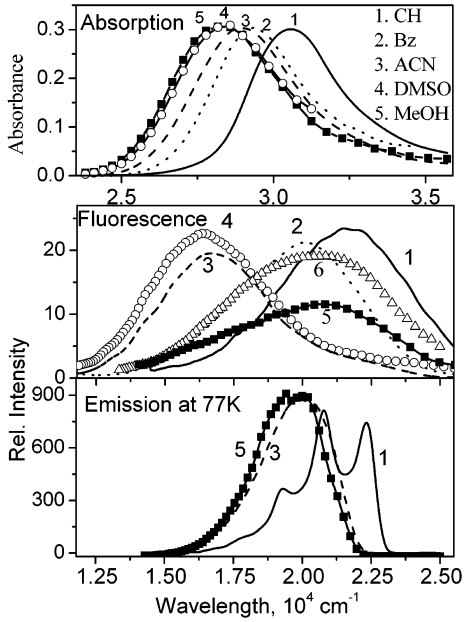

Figure 1. A. Ground-state absorption spectra of DMABP in cyclohexane (1), benzene (2), acetonitrile (3), DMSO (4), and methanol (5). B. Fluorescence spectra of DMABP in cyclohexane (1), benzene (2), acetonitrile (3), DMSO (4), methanol (5), and butanol (6). C. Total emission spectra of DMABP in MCH (1), acetonitrile (3), and methanol (5) matrixes at 77K. Both of the spectra are very similar in each of the solvent matrix.

fluorescence band are very sensitive to solvent characteristics. In aprotic solvents, the fluorescence maxima show large bathochromic shifts in more polar solvents (Table 1). The fluorescence maximum, which appears at 462 nm (21 645 cm^{-1}) in cycloheaxane, shifts to 602 nm (16 612 cm^{-1}) and 609 nm (16 420 cm^{-1}) in acetonitrile and DMSO, respectively. In addition, the Stokes shift ($\Delta\nu_s$) is also very large in each of the aprotic solvents. The Stokes shift values are about 9124 and 9291 cm^{-1} in cyclohexane and benzene, respectively, and 12 374 cm^{-1} and 12 151 cm^{-1} in acetonitrile and DMSO, respectively (see Table 1). However, in alcoholic solvents, e.g., in methanol and butanol, we observe the fluorescence maximum to appear at ca. 480 nm (20 833 cm^{-1}). The Stokes shift in alcohols is only 7336 cm^{-1}, which is even smaller than that in cyclohexane.

Quantum yields of fluorescence (ϕ_F), which have been determined by a comparative method using PABP in benzene as the standard ($\phi_F = 1.2 \times 10^{-3}$) using excitation wavelength at 355 nm, are given in Table 1.[33] ϕ_F is low in cyclohexane (on the order of 10^{-3}). It is even lower in acetonitrile and DMSO and nearly nonfluorescent in methanol. However, ϕ_F has been found to increase in normal alcoholic solvents with an increase

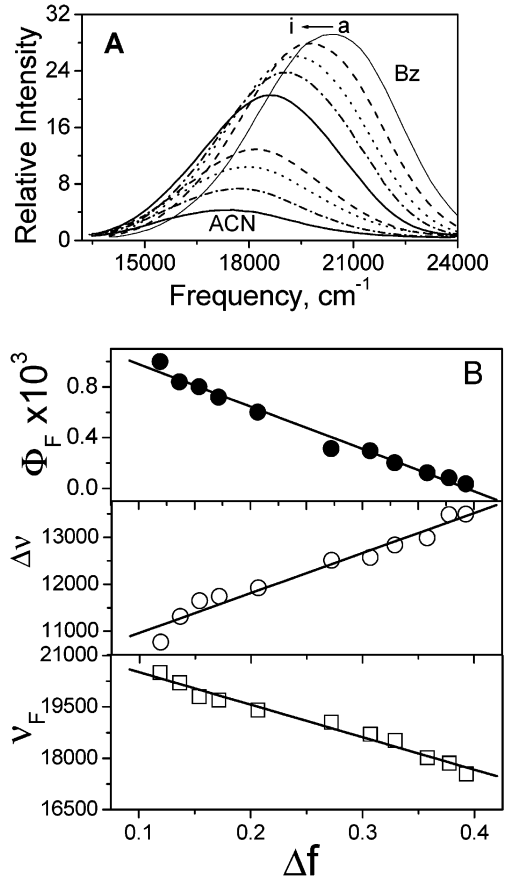

Figure 2. A. Fluorescence spectra of DMABP in benzene-acetonitrile mixed solvents with volume percentages of acetonitrile: a. 0, b. 10, c. 20, d. 40, e. 50, f. 70, g. 80, h. 90, and i. 100. B. Plot of the fluorescence quantum yield (ϕ_F) and Stokes shift ($\Delta\nu$) and fluorescence maximum (ν_F) vs Δf value of the solvent mixtures of benzene and acetonitrile.

in the chain length or the viscosity of the alcohols, e.g., ϕ_F is nearly double in butanol as compared to that in methanol.

The effect of polarity on the fluorescence spectra of DMABP has been investigated in benzene-acetonitrile as well as cyclohexane−ethyl acetate−acetonitrile solvent mixtures. The values of the dielectric constants and the refractive indices of the benzene-acetonitrile solvent mixtures of different compositions have been measured by Bakshi.[50] For the other solvent mixtures, the dielectric constants and the refractive indices were calculated assuming that the contribution of the individual solvents to the polarity parameter is proportional to the solvent composition. However, the dependence of ϕ_F and the Stokes shift ($\Delta\nu_s$) on solvent polarity have been seen to be similar in both kinds of solvent mixtures. The maximum of the fluorescence spectrum shifts gradually toward red due to increase in polarity of the solvent mixture. The plot of $\Delta\nu_s$ vs the solvent polarity function, Δf, called the reaction field parameter, defined by eq 1, is shown in Figure 2. The difference in dipole moment ($\Delta\mu$) between the fluorescing S_1 state and the ground (S_0) state has been calculated from the slope of the linear plot of $\Delta\nu_s$ vs Δf, using the Lippert−Mataga equation (eq 2).[51] By applying the partial volume addition method, as suggested by Edward, the Onsagar cavity radius, a, is estimated to be 3.56 Å.[52] Substituting the value of a, the value of $\Delta\mu$ has been determined to be 6.8 D. The theoretical value of the ground-state dipole moment (μ_g = 5.4 D) has been obtained by geometry optimization using the Hartee-Fock method with the 6-31G(d, p) basis set in the Gaussian 92 program. Hence, we obtain the value of the dipole moment of the excited state, μ_e, which is 12.2 D. We have also used eq 3 to determine the value of μ_e by using the variation of fluorescence energy (ν_F) as a function of the polarity parameter, Δf, and we obtain the value of μ_e, (11.5 D), which is nearly in agreement with that obtained from the solvent polarity effect on the Stokes shift (eq 2)

$$\Delta f = \frac{D - 1}{2D + 1} - \frac{n^2 - 1}{2n^2 + 1} \tag{1}$$

$$\Delta\nu_S = \frac{2(\mu_e - \mu_g)^2}{hca^3}\Delta f + \text{constant} \tag{2}$$

$$\upsilon_F = (2(\mu_e - \mu_g)\mu_e/hca^3)\Delta f + \nu_F^0 \tag{3}$$

Figure 1C shows the total emission spectra of DMABP (i.e., both the fluorescence as well as the phosphorescence spectra are combined together) recorded in methylcyclohexane (MCH), acetonitrile, and methanol matrixes at 77 K. Although MCH and methanol form good glassy matrixes at 77 K, acetonitrile forms a snow-type matrix only. However, emission from the surface of the sample in acetonitrile frozen in a quartz tube of 3 mm diameter could be collected very conveniently. The emission spectrum with well-resolved vibronic bands in the MCH matrix is very similar to the phosphorescence spectrum of benzophenone.[30] Comparison of the total emission spectrum in an acetonitrile matrix at 77 K with that recorded in solution at room temperature shows that the fluorescence emission band with a maximum at ca. 610 nm, which is seen in the room-temperature spectrum, is absent in that recorded in rigid matrix at 77 K. In methanol, the region of the total emission spectrum overlaps well with that of the fluorescence emission recorded in solution at room temperature. However, the long tail in the 600−750 nm region is not observed in the spectrum recorded in rigid matrixes at 77 K. The intensity of emission increases by about 2 orders of magnitude more in solid matrixes than that in solution at room temperature.

The nature of the total emission spectra, i.e., the shape and the position of the band maxima, did not change significantly while the chopper was used to chop the fluorescence emission. This suggests that, even in rigid matrixes at 77 K, fluorescence emission is weak but the phosphorescence emission is quite strong. Hence, the emission spectra presented in Figure 1C could be attributed to the phosphorescence emission of DMABP. It is important to note that phosphorescence emission is strong in the methanol matrix at 77 K despite a negligible triplet yield in this solvent at room temperature (see section 3.2). The phosphorescence spectrum in MCH is structured and has the higher energy onset at 432 nm, which corresponds to the triplet energy of 46.1 kcal mol^{-1}. The phosphorescence spectra in acetonitrile and methanol are broad having a single band and in both the cases the higher energy onset is at 450 nm, which corresponds to the triplet energy of 44.1 kcal mol^{-1}. These observations suggest that the nature of the triplet state in polar solvents is different from that in nonpolar solvents and the triplet energy level is significantly lower in polar solvents. The phosphorescence emission in MCH follows biexponential decay. The lifetimes of the two components are 3.8 and 40 ms. However, the phosphorescence emission is single exponential in methanol having a lifetime of about 95 ms. Phosphorescence lifetimes, τ_{Ph}, measured in solid matrixes of different solvents are given in Table 1.

3.2. Fluorescence Lifetime Measurement and Picosecond Laser Flash Photolysis Study. The fluorescence lifetimes of DMABP in various solvents have been measured using the time-

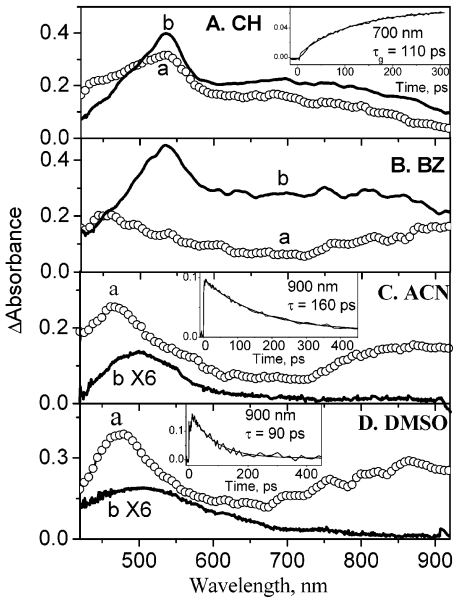

Figure 3. Transient absorption spectra recorded immediately (i.e., at 0 ps) (a) and at 6 ns (b) after photoexcitation of DMABP by 35 ps laser pulses of 355 nm in cyclohexane (A), benzene (B), acetonitrile (C), and DMSO (D). The insets show the temporal evolution of transient absorption monitored at 700 or 900 nm.

correlated single photon counting technique. In the time-domain above 40 ps, each of them has been fitted well by a single-exponential decay function, and the fluorescence lifetimes, τ_F, thus obtained are given in Table 1. τ_F values are short in aprotic solvents ($\tau_F \sim 100-160$ ps), except in benzene ($\tau_F \sim 900$ ps). In methanol, τ_F is shorter than the instrument response time ($\sim$40 ps) and hence could not be measured using this technique.

Figure 3 presents the time-resolved absorption spectra of the transient species produced due to photolysis of DMABP in various kinds of organic solvents using 355 nm pulses of 35 ps duration and recorded immediately, i.e., at 0 ps (a), and at 6 ns (b) after the laser pulse excitation. It is clearly evident from this figure that the spectral and decay characteristics of the transient species differ significantly in different solvents. In cyclohexane, the transient spectrum (a), recorded immediately after the laser pulse, has two major bands. One is weak but very broad occurring in the 600−930 nm wavelength region with no defined maximum. The other one occurs in the 420−600 nm region with a maximum at 530 nm. Although the features of the spectrum (b) recorded at 6 ns are not much different from those of the spectrum recorded at 0 ps, we observe a decay of absorption in the 400−500 nm region and a growth of absorption in the 600−900 nm region. The temporal profile of the transient absorption monitored at 700 nm shows the growth of the transient absorption with a growth lifetime of 110 ± 5 ps (inset of Figure 3A). This value is nearly equal to but a little longer than the fluorescence lifetime of DMABP in the same solvent (Table 1). In benzene, however, we observe the evolution of the spectral characteristics with time. The transient absorption spectrum in benzene recorded immediately after the laser pulse has the features which are distinctly different from those observed in the spectrum recorded at 6 ns in cyclohexane. The transient spectrum in benzene has two major absorption bands, one in the 600−930 nm region with maximum at ca. 900 nm and the other band in the 400−600 nm region with maximum at 450 nm. However, this spectrum evolves with time, and the spectrum recorded at 6 ns has features similar to those observed in the spectrum obtained in cyclohexane. The growth lifetime of the transient absorption monitored at 750 nm is about 1000 ps.

In acetonitrile, the transient absorption spectrum (a), recorded at zero ps, also has two major bands with maxima at ca. 470 and 880 nm. The absorbance values monitored at both of these wavelengths decay at the same rate and the lifetime of this transient has been determined by using 400 nm laser pulses of 50 fs duration for excitation, to be 160 ± 10 ps (inset of Figure 3C). After the decay of this transient, a new transient absorption spectrum (b), having a single band at ca. 500 nm, is evolved. In DMSO, the spectral characteristics of the transient species are very similar to those observed in acetonitrile. The decay lifetime of the short-lived transient in this solvent is about 90 ± 5 ps (inset of Figure 3D). We could not observe any transient absorption in methanol in the time-domain above 35 ps.

Comparing the values of the fluorescence lifetimes of DMABP with the decay or the growth lifetimes of the transient absorption measured in the corresponding solvents, the time-resolved spectra recorded at 0 and 6 ns after the laser pulse excitation could be assigned to the excited singlet and triplet states, respectively. Assignment of the spectra recorded at 6 ns after the laser pulse in different solvents has been confirmed by the laser flash photolysis study in nanosecond time-domain. The characteristics of the spectrum recorded at 6 ns in picosecond flash photolysis experiments are found to be similar to those in the spectrum recorded at 100 ns in the nanosecond flash photolysis experiment. The identity of the triplet spectrum was also confirmed by observing energy transfer from the triplet of DMABP to the triplet states of other known molecules, such as β-carotene. Quantum yields of triplet formation (ϕ_T) have been determined by using the comparative method and benzophenone as the standard ($\phi_T = 1$, λ_{max} of triplet absorption is at 525 nm).[2−4] The values of ϕ_T and τ_T (triplet lifetime) of DMABP in different solvents are given in Table 1. In cyclohexane, the intersystem crossing process is very efficient ($\phi_T = 0.92$) as compared to that in other solvents. However, τ_T follows the reverse trend. τ_T is much shorter in cyclohexane than those in other solvents.

The lifetime of the S_1 state of DMABP in cyclohexane could be obtained by multiplying the growth lifetime (110 ps) of the triplet absorption by ϕ_T, and this value (101.2 ps) agrees well with the fluorescence lifetime (Table 1). Table 1 also shows that the rate constant of the nonradiative process (k_{NR}) is larger by more than 2 orders of magnitude than that of the radiative process (k_R) in each of the aprotic solvents. k_{NR} is significantly larger in methanol.

3.3. Femtosecond Laser Flash Photolysis Study. We have studied the early time dynamics of the photophysical processes of DMABP in different aprotic and protic solvents of varying polarities and viscosities using 400 nm laser pulses of 50 fs duration for excitation and monitoring the transient absorption profile at different wavelengths in 470−1000 nm wavelength region at 20 nm intervals with about 120 fs time resolution. A few typical temporal absorption profiles recorded due to photoexcitation of DMABP in acetonitrile are shown in Figure 4. The time-resolved transient absorption spectra have been constructed using these temporal absorption profiles and six chosen time-windows are presented in Figure 5. The spectrum (curve a) constructed for 0.2 ps time window consists of only one major absorption band in the 600−800 nm wavelength region with a maximum at ca. 670 nm. The temporal absorption profiles, monitored at different wavelengths in this region, show an initial growth within the instrument response time ($\sim$120 fs) and then decay in ultrafast time scale with lifetime of about

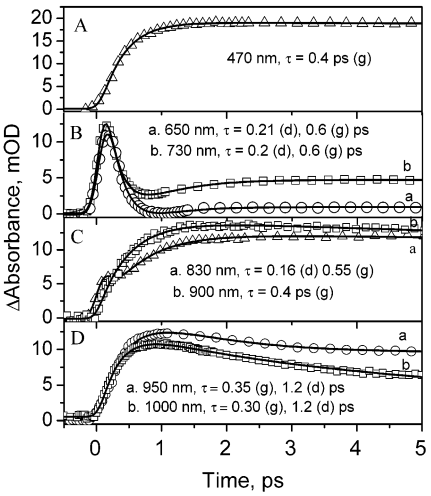

Figure 4. Temporal evolution of transient absorption monitored at different wavelengths following photoexcitation of DMABP in acetonitrile by 400 nm laser pulses of 50 fs duration. Solid lines represent the best triexponential fit functions. Lifetimes of two shorter components (growth (g) or decay (d)) are shown in the insets. The longest decay component (τ_3(d), Table 2), which has been fixed during the fitting process, is not shown in the insets.

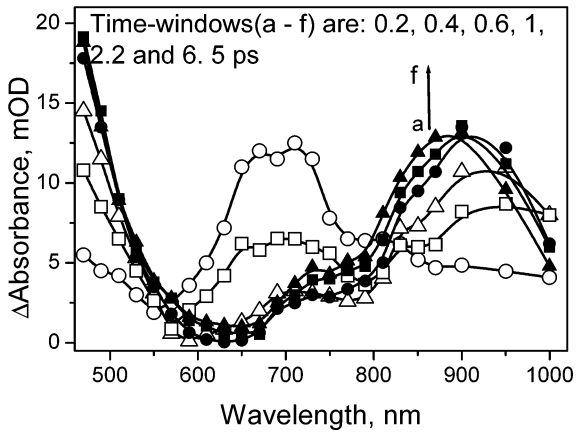

Figure 5. Time-resolved transient absorption spectra obtained following photoexcitation of DMABP in acetonitrile by 400 nm laser pulses of 50 fs duration. These have been constructed using the temporal profiles monitored in the 470−1000 nm region (a few of which have been presented in Figure 4).

0.20 ps. This is followed by a further growth of absorption with a growth lifetime of about 0.6 ps. Two typical temporal absorption profiles, recorded at 650 and 730 nm, have been shown in Figure 4B. The time-resolved transient absorption spectra (curves b−f in Figure 5) constructed for the later time-windows reveal the ultrafast decay of the band in the 600−800 nm region with concomitant development of two absorption bands in the 470−600 and 800−1000 nm wavelength regions.

One typical temporal profile presented in Figure 4A shows the growth of the absorption band in the 470−600 nm wavelength region and four of those for the wavelength region 800−1000 nm are presented in Figure 4, parts C and D. In the 470−600 nm wavelength region, we observe only the growth of the transient absorption with a growth lifetime of 0.4 ± 0.1 ps. However, the shape of the temporal profiles recorded in the 800−1000 nm region is sensitive to wavelength. The temporal profile recorded at 830 nm could be fitted by a function having three exponential terms. Before the decay of the transient species (lifetime is about 0.16 ps), which initially grows with the instrument response time, is complete, the absorption due to another species starts growing with the growth lifetime of about 0.55 ps. The latter decays with a longer lifetime, which has been determined to be 160 ps (Figure 3C). The lifetime of this longer decay component, which has been associated with each of the temporal absorption profiles presented in Figure 4, has not been shown in any of the insets of this figure but only two shorter components. The temporal absorption profile recorded at 900 nm shows the presence of a single growth component. In addition to the long decay component, we also observe the presence of an additional decay component at 950 and 1000 nm following the initial growth of the transient absorption. The lifetime of the growth component is wavelength dependent, and it decreases as the probe light of longer wavelength is used to probe the transient absorption within the 800−1000 nm absorption band (Figure 4, parts C and D). As a result, we observe a continuous blue shift of the maximum for the time-resolved spectrum in the 800−1000 nm region recorded at later time windows. The maximum of this band is observed to appear at ca. 950 nm at 0.4 ps. However, at later time windows, as the absorbance in this band continues to increase up to 5 ps, the maximum wavelength shifts gradually toward the shorter wavelength region, and the spectrum constructed at 5 ps shows the absorption maximum at ca. 850 nm.

To confirm the fact that whether the ultrafast decay component with lifetime of about 0.20 ps, which is very close to our instrument response time (0.12 ps), truly represents the dynamics related to the excited state of DMABP and not due to any kind of coherent artifact because of interaction between the pump and the probe pulses or either of these two pulses and the quartz windows of the sample cell, we performed the transient absorption experiment only with the solvent. This experiment showed no transient absorption signal but only zero baseline. We also performed the transient absorption experiments with different concentrations of the solute in acetonitrile. The nearly identical nature of the signal obtained with a sample solution having 10 times less solute concentration to that obtained with a higher concentration of the solute indicated that the dynamics within the 10 ps time-domain did not arise due to any kind of phenomena related to aggregation of the solute.

Figure 6 displays the temporal absorption profiles for the transient species produced due to photoexcitation of DMABP in three other aprotic solvents, namely, cyclohexane, benzene, and DMSO. The DMABP molecule in nonpolar solvents is not convenient for this study due to two reasons. DMABP is not very soluble in nonpolar solvents, and the absorption spectrum is shifted too far to the blue for efficient excitation at 400 nm. In cyclohexane, we could monitor the transient absorption signals only at a few selective wavelengths (e.g., at 470, 670, and 900 nm) with difficulty. Both of the transient absorption profiles monitored at 470 and 900 nm show a component growing up to about 5 ps with the growth lifetime of 1.1 ps. However, the transient absorption at 670 nm grows to a maximum within the instrument response time, but that does not show any kind of evolution and remains constant within 10 ps time-domain. The absence of decay of the transient absorption at 670 nm is possibly due to overlapping of the absorption band due to the S_1 state with that due to the T_1 state.

In benzene, the transient absorption signal monitored at 670 nm grows initially with the instrument response time and subsequently decays with a lifetime of 0.8 ps to show a residual absorption in the 5 ps time-domain. However, the latter increases further with a very long rise-time (∼900 ps) in a few hundred picosecond time-domain (not shown in the figure). While monitored at 900 nm, the growth lifetime of the transient

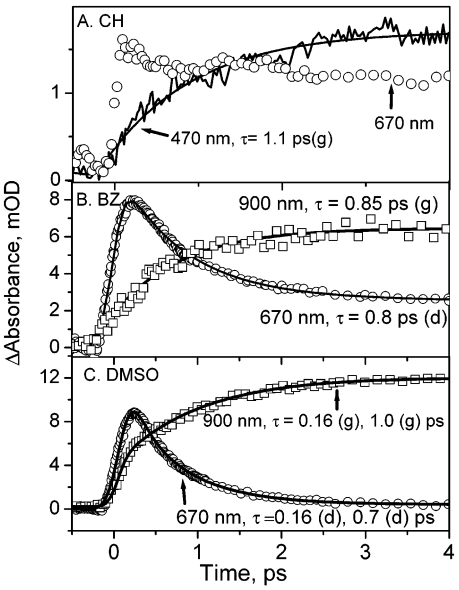

Figure 6. Temporal evolution of transient absorption monitored at 670 nm (a) and 900 nm (b), following photoexcitation of DMABP in cyclohexane (A), benzene (B), and DMSO (C), by 400 nm laser pulses of 50 fs duration. Solid lines represent the best fit-functions. Lifetime-(s) of the shorter component(s) (growth (g) or decay (d)) components are shown in the insets. The longest decay component (τ_3(d), Table 2), which has been fixed during the fitting process, is not shown in the insets.

absorption has been found to be 0.85 ps. In DMSO, the transient absorption profile at 900 nm grows biexponentially, with the components having the growth lifetimes of 0.16 and 1.0 ps. The final decay of this transient absorption takes place in a much longer time-domain, and the lifetime of this component has been determined to be 100 ps (inset of Figure 3D). At 670 nm, we observe biexponential decay of the transient absorption with lifetimes of 0.16 and 0.7 ps. These lifetimes have been presented in Table 2. The assignments of the components with different lifetimes will be evident during the course of further discussion.

We have also investigated the ultrafast dynamics of the excited states of DMABP in linear alcohols following photoexcitation at 400 nm. Figure 7 presents the time-resolved transient absorption spectra of DMABP in 1-butanol. The spectrum recorded immediately after the excitation laser pulse, i.e., at 0.2 ps, has the main absorption band in the 600−800 nm region with maximum at ca. 700 nm. This feature is similar to that observed in acetonitrile (curve a in Figure 5). However, in addition to this feature, a stimulated emission band in the 470−550 nm region is also observed in the transient spectrum recorded immediately after photoexcitation of DMABP in butanol. Both the absorption as well as the stimulated emission bands disappear rapidly with concomitant development of a new but weak absorption band in the 800−1000 nm region along with a shoulder band in the 650−750 nm region. The new band in the 800−1000 nm region also disappears after about 40 ps, but the residual absorption in the 470−800 nm region survives for longer time and hence we find a new absorption band with maximum at ca. 710 nm after about 40 ps (curve l in Figure 7B).

Figures 8−10 display the temporal absorption profiles monitored at 490, 670, and 900 nm in different normal alcohols. In each of the alcoholic solvents, the stimulated emission signal measured at 470 or 490 nm grows with the instrument rise time. In methanol, we observe the decay of the stimulated emission along with the simultaneous growth of the positive absorption with a lifetime of about 0.29 ps (Figure 8A). The decay dynamics of the stimulated emission in butanol and decanol have also been monitored at 490 nm (Figures 8B and C). We observe the presence of an ultrafast component for the stimulated emission decay (the lifetimes are 0.3 and 0.42 ps in butanol and decanol, respectively) and a longer component, which arises due to the decay of the stimulated emission and simultaneous growth of the positive absorption, with the lifetimes of 2.0 and 6.6 ps in butanol and decanol, respectively. The positive absorption decays in a longer time-domain.

In methanol, the transient absorption profile recorded at 670 nm (Figure 9a) shows an ultrafast decay with the lifetime of 0.22 ps to reach a small residual absorption within 1 ps. At 900 nm, the transient absorption grows with the same lifetime to reach the maximum within 1 ps (Figure 9A) and then decays at a longer time-domain with the lifetime of 5.2 ps. (Figure 10). In other alcohols, the absorption profiles, recorded both at 670 and 900 nm (Figure 9), could be fitted with the triexponential decay functions and the lifetimes of these components are given in Table 2 in terms of three decay-time constants, τ_1^a(d), τ_2^a(d), and τ_3^a(d), for the temporal absorption profiles recorded at 670 nm and two growth and one decay-time constants, τ_1^b(g), τ_2^b(g), and τ_3^b(d), respectively, for those at 900 nm. The actual value of τ_3^b(d) has been obtained by single-exponential fitting of the decay of the transient absorption recorded at 900 nm in the longer time-domain in the corresponding solvent (Figure 10). The value of τ_3^b(d) has been fixed to fit the transient absorption profile recorded at 900 nm in the shorter time-domain using a triexponential fit function consisting of two growth and one decay components (Figure 9). The same value has also been used as τ_3^a(d) in fitting the decay profiles recorded at 670 nm. The third component, τ_3^a(d), is longer lived and does not show any decay in the shorter time-domain, and hence, it represents a small residual absorption in these temporal absorption profiles. The growth lifetimes, τ_1^b(g) and τ_2^b(g), measured at 900 nm are nearly equal to those of the decay lifetimes, τ_1^a(d) and τ_2^a(d), measured at 670 nm in the corresponding alcohol. τ_1^a(d) or τ_1^b(g) represents an ultrafast decay component having a lifetime in the range of 0.2−0.46 in different kinds of solvents. Both τ_1^a(d) and τ_1^b(d) increase with an increase in chain length or viscosity of the alcohols. The presence of this ultrafast component becomes more evident in alcohols having longer chain length or higher viscosity. The lifetime of the second component, τ_2^a(d) or τ_2^b(g), also becomes longer in the solvents of higher viscosities. Table 2 also presents the physical parameters related to different solvents, along with the lifetimes of the transient species produced due to photoexcitation of DMABP.[53, 54]

We have followed the dynamics of transient absorption at 670 nm in butanol in the time-domain above 10 ps. The inset of Figure 10 shows the temporal dynamics in butanol (curve c) monitored at 670 nm. After the initial fast decay with the lifetime of about 1 ps (this decay in the 10 ps time-domain has been shown in Figure 9c), the transient absorption after 10 ps shows a small growth with the growth lifetime of 28 ps followed by a decay with the lifetime of about 60 ps.

4. Discussion

4.1. Nonradiative Process and Conformational Relaxation. Ground-state absorption characteristics of benzophenone and its amino substituted derivatives have been well characterized by several groups earlier.[26−28,31,32] In nonpolar solvents, say cyclohexane, the absorption band with a maximum at 325 nm has been assigned to the $\pi\pi^*$ transition. In more polar solvents, we observe a large bathochromic shift of this band and also the

TABLE 2: Lifetimes of Different Components in the Relaxation Dynamics of DMABP

				lifetimes, ps (measured at 670 nm)			lifetimes, ps (measured at 900 nm)		
solvent	ϵ	η	$\langle\tau\rangle_{solv}$[a]	τ_1[a](d)	τ_2[a](d)	τ_3[a](d)	τ_1[b](g)	τ_2[b](g)	τ_3[b](d)
CH	2.02	0.98		1.1	(growth at 470 nm)				
benzene	2.28	0.60	2.1		0.8			0.85	900
ACN	37.5	0.34	0.26		0.2			0.55[b]	160
DMSO	46.6	2.0	1.79	0.17	0.7		0.16	1.0	90
MeOH	32.7	0.55	5		0.22	5.2		0.22	5.2
1-propanol	19.92	1.94	26	0.20	0.55	25	0.20	0.6	25
1-butanol	17.5	2.6	63	0.26	0.95	32	0.25	1.03	32
1-pentanol	13.9	3.56	103	0.35	1.85	60	0.34	1.93	60
1-octanol	10.34	6.13		0.42	3.11	136	0.41	3.15	136
1-decanol	13.8	11	259	0.46	4.7	196	0.45	4.5	196

[a] ϵ and η (cP) values are taken from the following ref 53 and $\langle\tau\rangle_{solv}$ values are from ref 54. In the fitting procedure for the temporal absorption profiles recorded at 670 nm, the lifetime of the longest component was kept fixed at the value of τ_3[b](d). d or g inside the bracket along with τ indicates that the particular component represents decay or growth component. [b] Measured at 830 nm. Percentage of error involved in the measurement of different lifetimes are less than 5%.

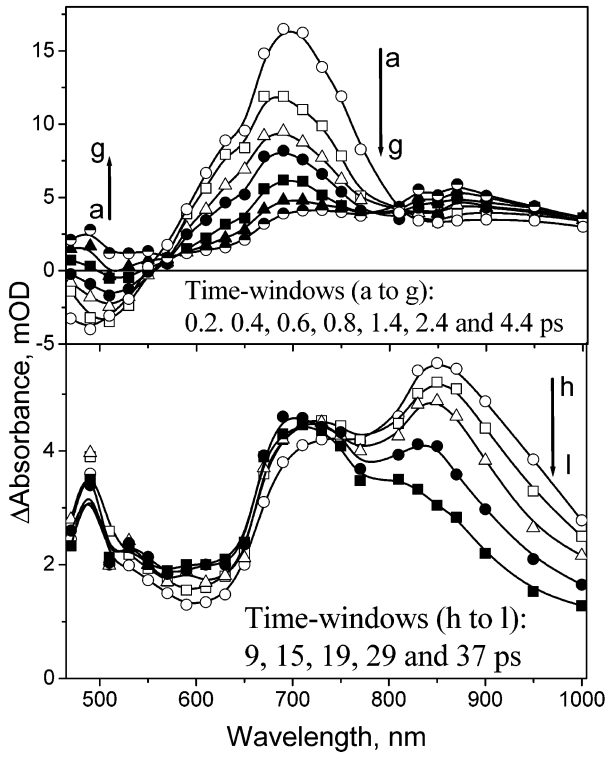

Figure 7. Time-resolved transient absorption spectra obtained following photoexcitation of DMABP in butanol by 400 nm laser pulses of 50 fs duration. These have been constructed using the temporal profiles monitored in the 470−1000 nm region (a few of which have been presented in Figures 8−10).

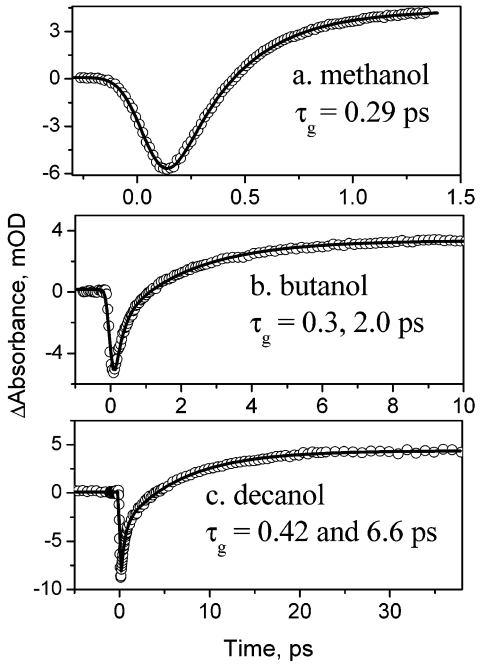

Figure 8. Temporal evolution of transient absorption monitored at 470 nm following photoexcitation of DMABP in different normal alcohols by 400 nm laser pulses of 50 fs duration. Solid lines represent the best fit functions. Lifetimes of the decay (d) or growth (g) components have been shown in the insets. The shortest growth component represents the decay of stimulated emission, which is followed by further growth due to increase in transient absorption.

appearance of a small shoulder at 310 nm. In nonpolar solvents, due to energetic proximity of the nπ^* and $\pi\pi^*$ states, the absorption bands due to these transitions are overlapped, but with an increasing polarity of the solvents, the energy level due to the $\pi\pi^*$ state comes down with respect to that due to the nπ^* state. Thus, the presence of both of the bands becomes evident in polar solvents. A large shift of the absorption maximum in polar solvents suggests a higher polarity of the excited state as compared to that of the ground state. This conclusion is supported by the large value of the excited-state dipole moment ($\mu_e \sim 12$ D) determined from the fluorescence spectroscopic data. The asymmetrically charge-distributed S_1 ($\pi\pi^*$) state gains the intramolecular charge transfer (ICT) character in highly polar solvents, such as acetonitrile and DMSO.[30−32] A larger red shift and larger bandwidth in methanol could be assigned to the strong intermolecular hydrogen bonding interaction between the ICT state and the solvent.

Low fluorescence quantum yields and the short excited-state lifetimes of DMABP in solutions are direct indications of the nonradiative processes being dominant in the excited-state relaxation process of DMABP (Table 1). Absence of the low energy fluorescence band in the room-temperature fluorescence spectrum as well as very high yield of phosphorescence emission in polar solvents, while the triplet yield measured at room temperature is negligible, suggests that there exists an efficient nonradiative deactivation pathway, which involves a change of molecular conformation in the S_1 state. Table 1 shows that the nonradiative internal conversion process is much more efficient than the radiative decay or the intersystem crossing (ISC) process taking place in solutions at room temperature. In nonpolar solvents, however, the large quantum yield of the triplet indicates that the ISC process is the major deactivation pathway. In polar aprotic solvents, both ϕ_F and τ_F decrease as well as the rate of the internal conversion process (k_{IC}) increases with an increase in polarity (Figure 2B and Table 1). Surprisingly, ϕ_F

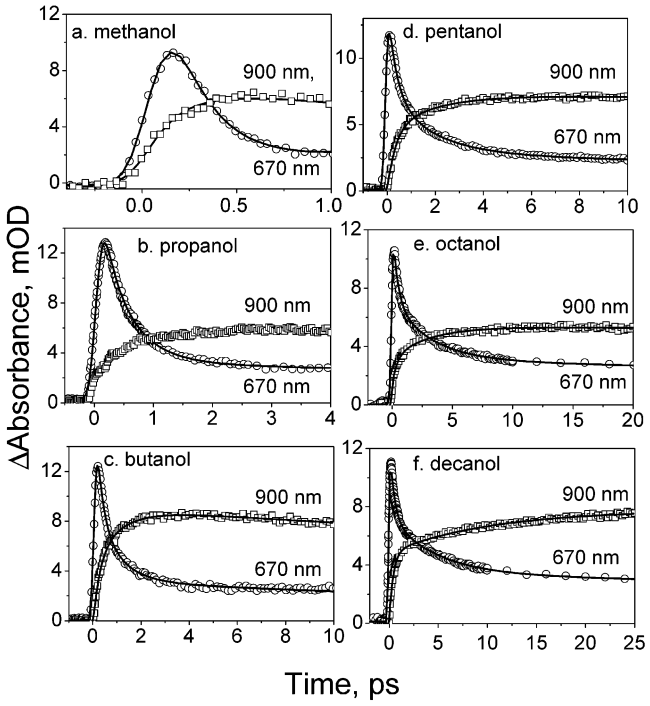

Figure 9. Temporal evolution of transient absorption monitored at 670 and 900 nm following photoexcitation of DMABP in different normal alcohols by 400 nm laser pulses of 50 fs duration. Solid lines represent the best triexponential fit functions. The lifetimes of different decay (d) and growth (g) components have been given in Table 2.

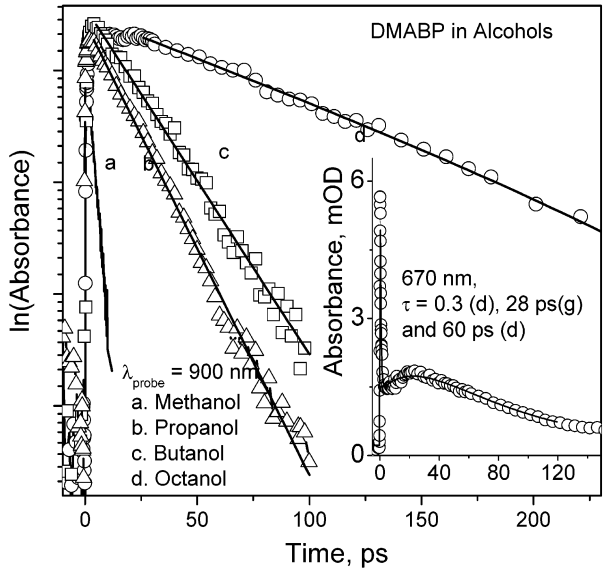

Figure 10. Decay dynamics of the S_1(TICT) state in alcohols monitored at 900 nm. Lifetimes (τ_3^b(d)) obtained by single-exponential fitting of the decay profiles are given in Table 2. Inset: Decay dynamics of the transient absorption in 1-butanol monitored at 670 nm.

is about six times larger and τ_F is also much longer in benzene as compared to those in cyclohexane. It possibly suggests that in this solvent the $\pi\pi^*$ state, which is a higher energy state lying above the $S_1(n\pi^*)$ state in cyclohexane, comes down below the latter and becomes the S_1 state. Benzene, despite having the dielectric constant (2.28), which is not very different from that of cyclohexane (2.02), acts as a microscopically polar solvent due to its large quadruple moment.

We observe a few distinct differences in the properties of the S_1 state in aprotic and protic (or alcoholic) solvents. The Stokes shift values are very large (>9000 cm^{-1}) in aprotic solvents as compared to those in protic solvents. The Stokes shift in methanol is 7336 cm^{-1}, which is even smaller than those in nonpolar aprotic solvents (Table 2). This possibly suggests that in aprotic solvents the conformational geometry of the fluorescing S_1 state is appreciably different from that of the Franck−Condon (FC) state. In the rigid matrix of acetonitrile, we do not observe the emission band with a maximum at 600 nm that is observed for the same sample in solution at room temperature. In a rigid matrix, the molecular motions are frozen, and the emission process is likely to occur from the FC or LE state, which is the un-relaxed conformation of the molecule in the S_1 state. It is also important to note that in the rigid matrix of acetonitrile, phosphorescence emission occurs in the wavelength region, which is blue shifted as compared to that of the fluorescence spectrum (Figure 1). Hence, all of these observations suggest that in aprotic solvents the fluorescence emission takes place mainly from a conformationally relaxed S_1 state of the molecule. On the other hand, in alcohols, a smaller Stokes' shift than those in aprotic solvents is indicative of the fact that the geometry of the S_1 state, which has fluorescence maximum at 480 nm, is not significantly different from that of the ground state and this fluorescence emission must be taking place from the LE state. However, the fluorescence spectra recorded in alcoholic solvents at room temperature show a long tail, having very weak intensity in the red side of the maximum emission wavelength, extending up to about 800 nm. This long tail could possibly be assigned to the emission from the conformationally relaxed state. We also observe a long tail in the blue side of the maximum of the room-temperature fluorescence spectra in polar aprotic solvents. These facts suggest that fluorescence emission with a maximum at 480 nm in alcohols and at ca. 610 nm in acetonitrile and DMSO may mainly be originating from the unrelaxed and relaxed conformers in alcohols and aprotic solvents, respectively. Long tails in the fluorescence spectra arise due to emission from the other conformer(s), which is (are) formed during the course of the relaxation process. In other words, the S_1 state of DMABP shows the features of dual emission and both the LE and TICT states are emissive. However, due to the differences in the deactivation mechanism of the S_1 state in different kinds of solvents, the emission maximum arises from emission due to either the LE state in alcohols or the conformationally relaxed state in aprotic solvents. In alcohols, very short lifetimes of the S_1 state, strong dependence of the lifetimes on viscosity (Table 2), as well as very large nonradiative decay rates (in methanol the k_{NR} value is about ~200 times larger than those in aprotic solvents) are indicative of the fact that very fast energy degradation via the intermolecular hydrogen bond stretching vibrations also play an important role in the deactivation process along with the intramolecular conformational relaxation processes. [55, 56]

4.2. Mechanism of Conformational Relaxation. Geometry optimization for the ground state by the Hartee-Fock method with the 6-31G(d,p) basis set using the Gaussian 92 program shows that the dihedral angle between the phenyl plane of the dimethylaminophenyl moiety and the carbonyl group of the DMABP molecule is about 22° and with the two halves of the molecule having initial dihedral angle of about 55° (Scheme 2). The nitrogen atom and two carbon atoms of the dimethylamino group are lying on the plane of the phenyl ring to which the dimethylamino group is attached. For the majority of the simple organic molecules containing the electron donating and accepting moieties, the charge separation is more favorable in a twisted conformation, i.e., if the molecular planes of the two moieties are positioned nearly at the mutually perpendicular

SCHEME 2: Optimized Geometry of the Ground State of DMABP

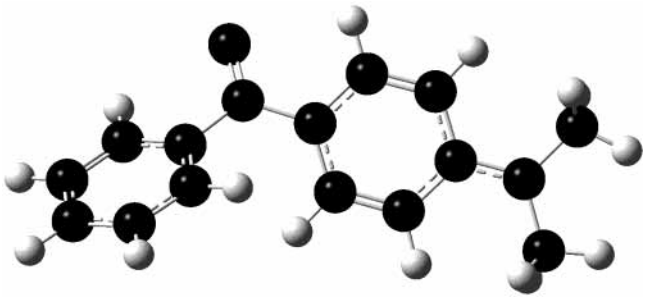

configurations with respect to each other.[35,57−59] The reason for the possibility of an energetic minimum has been assigned to the nearly-complete orbital decoupling at the perpendicular geometry leading to bi-radicalloid character of the corresponding excited state, if the interaction with the other states (e.g., of mesomeric character) is not strong.[57,58] The minimum free energy structure is a compromise between the dipolar stabilization and the mesomeric interaction. In polar solutions, the configuration with the maximum dipole moment is preferentially stabilized, so that for strong dipolar stabilization and weak mesomeric interaction, the lowest excited state corresponds to the twisted structure.[57, 58]

The 400 nm excitation laser pulse creates a population in the FC region of the S_1 state potential energy surface (PES) of DMABP. In the FC region, the molecule has a conformation similar to that of the ground state. This is a $\pi\pi^*$ state in nonpolar solvents or an ICT state in polar solvents. According to the free energy scheme, population motion should take place along the reaction coordinate, to attain the more stable geometry with the two halves orthogonally oriented with each other.[35] Hence, the reaction coordinate should have a predominant contribution from the twisting of the phenyl groups. Additionally, in polar solvents, the surrounding solvent dipoles require reorganization and reorientation around the newly created more polar S_1 state of ICT character, to attain a new arrangement of solvent dipoles around it, which is known as solvation. Hence, we expect to observe mainly two kinds of relaxation processes following photoexcitation of DMABP: (i) solvation and/or population spreading in the FC region to attain an excited state having a pre-twisted geometry (this has been designated as the LE state) and (ii) twisting of the dimethylaminophenyl group with respect to the carbonyl group to attain a post-twisted geometry, which is normally designated as the TICT state. Both solvation and twisting processes may possibly be proceeding simultaneously after creation of the excited state. However, in nonpolar solvents, the solvation process is expected to play a minor role in the relaxation dynamics of the S_1 state and the conformational change via twisting should be the major relaxation process.

4.3. Spectroscopic Properties of the LE and TICT States. The characteristics of the time-resolved transient absorption spectra (Figures 5 and 7) and the decay dynamics recorded at different wavelengths (Figures 4 and 6−10) clearly reveal the features of the relaxation dynamics of the S_1 state following a three-state model, in which the three states are referred to the electronic ground state and two adiabatically coupled electronic excited states.[41, 60] One of them, produced immediately following photoexcitation, is the LE state, having the conformation very similar to that of the ground state but larger dipole moment. The other is the conformatoinally relaxed TICT state, which is produced following the decay of the LE state. In the case of a "strong-coupling" limit, the relaxation dynamics is described

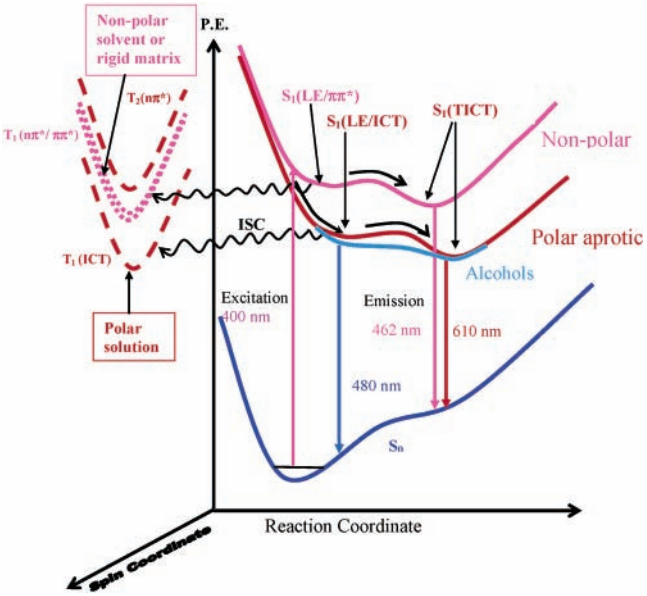

Figure 11. Potential energy surface (PES) diagram for the relaxation dynamics of the excited states of DMABP. S_1(LE) and S_1(TICT) represents the two adiabatically coupled locally excited and relaxed or twisted S_1 states, respectively. In nonpolar solvents, the LE state is an asymmetrically charge-distributed $\pi\pi^*$ state, but in polar solvents, the LE state is an ICT state. The LE to TICT conversion process via diffusive twisting of the dimethylaminophenyl group is associated with a barrier-crossing process. In alcoholic solvents, the height of the energy barrier is lower than that in aprotic solvents. In alcoholic solvents, the emission maximum at 480 nm arises due to emission from the S_1(LE) state but in aprotic solvents the emission maximum in the 462−610 nm region arises due to emission from the S_1(TICT) state. This diagram also presents the relative positions of different triplet energy levels and possible intersystem crossing processes in rigid matrixes at 77 K.

by a "two-state-two-mode" model, in which the LE and TICT states are considered to constitute a single S_1 state with two minima in the excited-state potential energy surface (Figure 11).[61]

The short-lived transient species, which is characterized by the absorption band in the 600−800 nm region in acetonitrile (curve a in Figure 5) or by the absorption band in the 600−800 nm region and a stimulated emission band in the 470−550 nm region in butanol (curve a in Figure 7), could be assigned to the LE state. This species undergoes a very fast twisting process to form the conformatinally relaxed TICT state. The transient absorption spectra with two absorption bands in the 470−600 and 650−1000 nm regions (curve f in Figure 5 and curve g in Figure 7) could be assigned to the TICT states. Now the blue shift of the absorption maxima of the 800−1000 nm band in the time-resolved absorption spectra in acetonitrile (Figure 5) may be revealing either the dynamics of solvation of the TICT state or the conformational relaxation process itself. Since acetonitrile is a "fast solvent" with a solvation time of about 0.26 ps (Table 2), the dynamic blue shift of the transient absorption maximum continuing up to about 5 ps could not be correlated with the solvation process.[54] Hence, the blue shift of the absorption maximum may possibly be correlated with the progress of the twisting process. Different molecular conformations, which are adopted by the molecule during the twisting process, may have different absorption maxima. Although the change of conformation of the molecule proceeds along the PES of the S_1 state from the region corresponding to the LE state toward that of the TICT state, the energy difference between the S_1 and S_n states possibly increases and hence the absorption

maxima of the $S_n \leftarrow S_1$ transition for the conformers formed at the later time-windows are gradually blue-shifted.

The simple three-state model for the excited-state relaxation dynamics predicts that the decay of the LE state should be followed by the growth of the TICT state, without the presence of any other intermediate. However, in acetonitrile, the decay lifetime of the LE state ($\tau_1^a = 0.20$ ps) monitored at 670 nm is apparently faster than the growth lifetimes measured at different wavelengths in the 800−1000 nm band, which has been assigned to the TICT state. Truly, the growth lifetime has been seen to be wavelength dependent, and it increases from 0.3 ps measured at ca. 1000 nm to 0.55 ps measured at 830 nm (Figure 4). This difference could be rationalized by the fact that the probe lights of different wavelengths monitor the different regions of the PES. The probe wavelength of 1000 nm, which is the longest wavelength accessible by our experimental set up, corresponds to the absorption maximum of a transient species, which has a conformation very similar to that of the LE state. We observe a fast growth of absorption followed by a decay component in the temporal absorption profile recorded at 1000 nm (Figure 4D). The fast growth component represents the formation of a conformer having the geometry corresponding to a particular region on the PES of the S_1 state, and the subsequent decay represents the change of its geometry forming another conformer corresponding to a lower energy region on the PES. The probe frequencies corresponding to the shorter wavelength side of the 800−1000 nm band monitor the evolution of the transient species having conformations similar to that of the TICT state, and hence, they show a longer growth of the transient absorption than those measured using the probe lights of longer wavelengths.

The absorption decay dynamics monitored in other solvents also reveal that molecular twisting is the dominant process for the relaxation of the S_1 state. We could not observe stimulated emission from either the LE or TICT state in aprotic solvents possibly due to overlapping of the transient absorption and stimulated emission bands. Hence emissive or nonemissive character of both the LE and TICT states could not be inferred from the time-resolved absorption experiments. However, in alcoholic solvents, we observe the appearance of a stimulated emission band immediately after photoexcitation and it follows the dynamics, which is very similar to that of the LE state monitored at 670 nm. Hence, it is quite justified to suggest that the stimulated emission band with a maximum at 490 nm is the characteristic of the LE state. However, the emissive or nonemissive character of the TICT state could not be confirmed from the results of the transient absorption experiments due to the same reason as in the case of the aprotic solvents.

Hence, it is evident that the early-time dynamics observed in the present work (Figures 4−9) represents mainly the dynamics of conversion from the LE state to the TICT state in all kinds of solvents. The lifetimes of two short decay components, τ_1^a(d) and τ_2^a(d), determined at 670 nm agrees well with those of the corresponding growth components, τ_1^b(g) and τ_2^b(g), obtained at 830 or 900 nm. Both the lifetimes increase with an increase in viscosity of the solvent, although the dependence is different (see section 4.4). In methanol and acetonitrile, the temporal profiles at 670 and 900 nm could be well fitted by a dual exponential decay function, probably because of similar lifetimes of these shorter components. In benzene also, the decay of the LE state and the growth of the TICT state could be fitted by single-exponential functions. In cyclohexane, the growth of the transient absorption with the lifetime of 1.1 ps could be assigned to the rate of conversion of the LE state to the TICT state. Following the above discussion, the schematic PES diagram for the relaxation dynamics of the S_1 state of the DMABP molecule, both in nonpolar and polar solvents, has been represented in Figure 11. The origin of the different components will be discussed in the following sections.

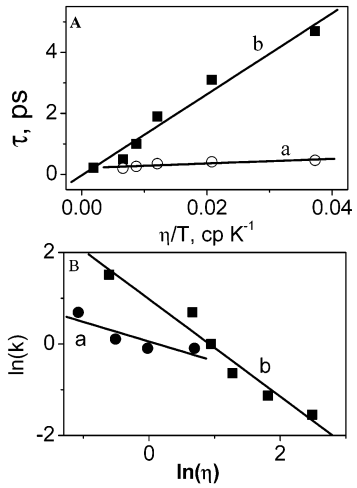

Figure 12. A. Plots of τ_1(a) and τ_2(b) in alcohols against η, following the Stokes−Einstein−Debye relation (4). Slopes of the best-fit linear functions are 7.5×10^{12} and 1.3×10^{14} s K cP^{1-}, respectively. B. Plots of $\ln(\tau_2^b(g))^{-1}$ vs $\ln(\eta)$ in aprotic (a) and alcoholic (b) solvents revealing the linear relation between the two parameters following eq 6. Slopes of the best-fit linear functions are −0.43 and −1 in aprotic and alcohoic solvents, respectively.

4.4. Viscosity Dependence of the Relaxation Rates. Since the formation of the energetically stable TICT state should be associated with the diffusive rotational motion of either the dimethylamino group attached to one of the phenyl rings or the entire dimethylaminophenyl group attached to the benzoyl group (this aspect will be discussed in section 4.5), the viscosity of the solvent (η) is expected to influence the rates associated with the decay of the LE state monitored at 670 nm as well as those with the formation of the TICT state monitored at 900 nm. Table 2 shows that these rates are nearly equal (i.e., τ_1^a(d) $\sim \tau_1^b$(g) $= \tau_1$ and τ_2^a(d) $\sim \tau_2^b$(g) $= \tau_2$). According to the Stokes−Einstein−Debye theory, rotational diffusion time is related to the viscosity of the solvent by the relation 4

$$\tau_{rot} = (V/k_B T)\eta \qquad (4)$$

where V is the effective volume of the rotating group, k_B is the Boltzmann constant, and the temperature ($T = 295$ K) is also a constant. In Figure 12A, both of the lifetimes, τ_1 and τ_2, have been plotted against η. Although linear viscosity dependence is observed for both the components, the relative values of the slopes of the best-fit linear functions (7.5×10^{12} and 1.3×10^{14} s K cP^{-1} for the lines representing τ_1 and τ_2, respectively) reveal that the viscosity dependence of the ultrafast component, τ_1, is nearly negligible (slope is nearly 20 times smaller) as compared to that of the slower component, τ_2. A significant viscosity dependence of τ_2 suggests that this component must be originating from the rotational diffusion of the dimethylamino group or the dimethylaminophenyl group. The ultrafast component may not have arisen due to the twisting process but possibly have an origin other than that.

The most widely used model for the description of isomerization or conformational relaxation dynamics is that of Kramers.[62] Combination of his ideas with the recent calculations and the experimentally observed facts led to the formulation of an empirical power law expression, which fits all of the data for

the rate constants of isomerization or conformational changes and can be written in the form[63]

$$k_{iso} = \left(\frac{B}{\eta^a}\right) \exp\left(-\frac{E_{act}}{RT}\right) \quad (5)$$

Two terms in this functional form represent the contributions from two different factors controlling the isomerization or conformational relaxation rate. The first term (i.e., B/η^a, where B is a constant, and $0 \leq a \leq 1$) is a universal function of viscosity and represents the "friction" or the "dynamical" effects exerted by the surrounding solvent or medium opposing the motion of the parts of the molecule involved in the conformational relaxation process. The second term, $\exp(-E_{act}/RT)$, represents the "barrier" or "static" effects represented in the form of activation energy for the conformational relaxation process. At a particular temperature and in a particular class of solvents, in which E_{act} remains more or less unchanged, the exponential term may be considered as a constant factor and hence eq 5 may be written as

$$\ln(k_{iso}) = -a \ln(\eta) + C \quad (6)$$

A plot of $\ln(k_{iso})$ vs $\ln(\eta)$ should be a straight line with a negative slope with a magnitude equal to a and the intercept is equal to the constant, $C = \ln(B) - E_{act}/RT$. Figure 12B represents two such plots, which show the linear dependence of $\ln(\tau_2^{-1})$ vs $\ln(\eta)$ in two different classes of solvents: aprotic and protic. The existence of the barrier between the LE and the TICT states in the present system is evident from the linear logarithmic relation between the growth rate ($k_{iso} = 1/\tau_2$) of the transient species monitored at 900 nm, which represents the rate of formation of the conformationally relaxed S_1(TICT) state. In the case of the alcoholic solvents, a is nearly equal to unity, whereas in aprotic solvents, this value is 0.43. Fleming and Waldeck have made attempts to find out a correlation between E_{act} and the parameter a through a careful investigation of the results reported from the numerous studies performed on the isomerization reactions and conformational relaxation processes.[63,64] A few important points have emerged from these investigations. The most important one, which is relevant to our results, is that in the case of larger barrier height for photoisomerization or conformational relaxation process the rate for the same has a less strong dependence on viscosity of the solvents as measured by the value of a. Hence, the smaller value of a indicates a larger barrier for isomerization reaction. As the barrier gets smaller, the barrier crossing process is controlled by the "dynamical" interactions influenced by intramolecular motions via intermolecular exchange of energy and momentum. In this case, the bulk viscosity should govern the momentum transfer and hence the barrier crossing dynamics.[65] In the absence of any information regarding the value of E_{act} for the process of conformational change or the twisting process in DMABP, we could only make a comment that the height of the energy barrier for the twisting process in DMABP in aprotic solvents (for which the value of a is $\sim$0.43) is higher than that in the case of the alcoholic solvents (for which the value of a is near unity and the barrier is very low (or quasi-barrierless). The lower barrier height for the twisting process in the alcoholic solvents is possibly due to solvation of the transition state via intermolecular hydrogen bonding with the solvents.[66]

4.5. Twisting Dynamics. Two possibilities for the excited state twisting of the DMABP molecule can be suggested: (i) twisting of only the dimethylamino group or (ii) twisting of the dimethylaminophenyl group with respect to the benzoyl group. Recently, Glasbeek and co-workers investigated the ultrafast fluorescence dynamics of MK and 3,6-bis(dimethylamino)-10,10-dimethylanthrone (also called "blocked Michler's ketone", BMK), in which the two benzene rings have been fused to resist the twisting of the phenyl groups.[32] In this molecule, only the twisting of the dimethylamino group is possible but not that of the entire dimethylaminophenyl group. However, twisting of either the dimethylamino group or the entire dimethylaminophenyl group is feasible in MK. Distinct differences were observed in the excited state dynamics of MK and BMK. Twisting motion was completely absent in BMK, although the dimethylamino group of BMK was free to twist. Hence it was concluded that that the twisting of the dimethylaminophenyl group, rather than the twisting of only the dimethylamino group, was responsible for the conformational relaxation process in MK. Spectroscopic consequences of the excited-state relaxation dynamics of the DMABP molecule are very similar to that of MK and also to those of the nonradiative relaxation dynamics of TPM dyes.[39,40] In the case of TPM dyes, internal twisting through the torsional motion of the benzenic rings containing the dimethylaminophenyl groups has been found to be the dominant mechanism of the S_1 state relaxation dynamics. The torsional relaxation times of the benzenic rings of malachite green (MG) and crystal violet (CV) in DMSO have been reported to be 0.77 and 0.85 ps, respectively, by Mokhtari et al.[40] A comparison of these values with those presented by τ_2^a(d) or τ_2^b(g), in Table 2, led us to correlate these lifetimes with the twisting dynamics of DMABP. Hence, we conclude that the twisting of the dimethylaminophenyl group with respect to the benzoyl group is responsible for the observed transient behavior and is likely to be the major process in the excited-state relaxation dynamics of DMABP.

4.6. Origin of the Ultrafast Component. We have already indicated that the ultrafast components, τ_1^a(d) or τ_1^b(g), which have been observed in the excited-state relaxation dynamics of DMABP, may have an origin different from that due to the twisting process. Various origins may be proposed for this component. Mokhtari et al. observed a similar ultrafast decay component in the excited-state relaxation dynamics of CV and MG.[40] It has been shown that the relaxation dynamics follow multiexponential decay, and diffusive rotation of the dimethylaminophenyl rings has been found to be involved in the nonradiative deactivation process.[40] However, the ultrafast time constants of about 120 and 180 fs for MG and CV, repectively, in DMSO could not be attributed to the diffusive rotation of the dimethylaminophenyl groups but to the relaxation of the solvent perturbed intramolecular low-frequency vibrational modes.[39,40] The ultrafast process that we observe here in the case of DMABP is also solvent dependent. The lifetime of this ultrafast component increases from 0.22 ps in methanol to 0.46 ps in decanol. Although one can indeed expect that the high frequency or hard internal vibrational modes excited with small amplitude relax without solvent hindrance, the low-frequency modes may be perturbed by the solvent. Like the TPM dyes, the nonrigid DMABP molecule is also expected to have numerous active low-frequency modes and hence the relaxation of these modes may be attributed as a possible reason for the occurrence of the ultrafast component, τ_1^a(d) or τ_1^b(g).

The inertial solvation process can be another possible origin of the ultrafast decay or growth component observed in the excited relaxation dynamics of DMABP. As we mentioned earlier that the FC state produced following photoexcitation of DMABP is an ICT state, we expect the solvation process to follow photoexcitation. Table 2 presents the average solvation

times, $\langle\tau\rangle_{solv}$, in different solvents used in this work. These solvation times have been determined by Maroncelli and co-workers using a suitable fluorescent probe.[54] However, the ultrafast decay or growth time constants, $\tau_1{}^a$(d) or $\tau_1{}^b$(g), measured in different solvents in the present work are much shorter than the average solvation times in the corresponding solvents. Several recent studies on solvation dynamics have found a universal ultrafast component in the 50−100 fs range in many solvents.[67−71] The ultrafast component in solvation dynamics was first observed by using time-resolved dynamic fluorescence Stokes' shift method by Fleming and co-workers in acetonitrile, methanol, and water.[67−69] Such an ultrafast component in higher normal alcohols (ethanol−butanol) has been reported by Joo et al. in their studies of the solvation dynamics of a large dye molecule in these alcohols using three measurement techniques, namely, the three pulse photon echo shift measurement (3PEPS), the transient grating (TG), as well as the transient absorption techniques.[70] They have also found that the presence of such a component in alcohols is rather generic in nature and also the echo decay slows down with increasing chain length. Joo et al. have also shown both theoretically as well as experimentally that the transient absorption technique can reveal the features of ultrafast solvation dynamics, although the other two techniques, namely, TG and 3PEPS, are more reliable for this purpose.[70]

4.7. Solvation. A large difference in the dipole moment ($\Delta\mu$ = 6.8 D) between those of the fluorescing S_1 state and the ground state suggests that solvation dynamics should also contribute significantly to the relaxation dynamics of DMABP in polar solvents. Using the femtosecond fluorescence dynamic Stokes shift method, Glasbeek and co-workers showed that solvation of the ICT state plays an important role in the excited-state relaxation dynamics of MK. To describe the interplay between the intramolecular motions and the solvent relaxations processes observed in the case of dimethylaminobenzonitrile, several different two-dimensional kinetic models have been introduced.[72−75] Among them, models suggested by Nordio and co-workers (Nordio model) and by Hynes and co-workers (KH model) have been the most successful ones.[72,73,74] The kinetic experimental results can be satisfactorily fitted with different kinds of 2D models, e.g., those necessitating an activation barrier (KH model) and those not requiring it (Nordio model). It turns out that the major parameter determining the behavior of such kinds of systems is the time-scale of the solvent relaxation as compared to the intramolecular twisting motion of the molecule. It can be measured as the diffusive coefficient along the solvent coordinate (D_S) to that along the internal (or twisting motion) coordinate (D_R). A fast-solvent case ($D_S \ll D_R$) and a slow-solvent case ($D_S \gg D_R$) can be distinguished. For the latter case, nonexponential kinetics has been predicted. Additionally, solvation dynamics in the case of most of the solvents is nonexponential in itself and usually occurs on a time scale ranging from ~50 fs to several hundreds of picoseconds.[54,67−71] We mentioned earlier that we possibly observed the inertial or nondiffusive component of solvation of the ICT state, which is ultrafast and complete within a few hundred femtosecond. However, the aspects of nonexponential solvation dynamics have not yet been introduced into the model of Nordio and co-workers, and D_S can therefore be viewed as an averaged solvation parameter, ($\langle\tau\rangle_{solv}$) (Table 2) and mainly be represented by the diffusive component of solvation. For the case of slow solvents, e.g., alcohols with longer chain length, like octanol and decanol, and for a not-too-large barrier as in the case of DMABP, the Nordio model predicts that the molecule twists first and solvation follows the large-amplitude twisting motion. So, the diffusive component of solvation possibly accompanies and follows the conformational relaxation process, which is much faster than the solvent relaxation process (Table 2). In addition, Table 2 shows that the lifetime of the LE-TICT conversion process (τ_2) in all kinds of solvents, except acetonitrile, is shorter than the solvation time. We have not been able to identify and isolate this component of solvation from the conformational relaxation process in our experiments. However, in acetonitrile, which is a "fast-solvent", τ_2 is very close to the average solvation time. Hence, in this solvent, solvation and twisting processes are simultaneous and the latter is possibly controlled by solvation of the ICT state.

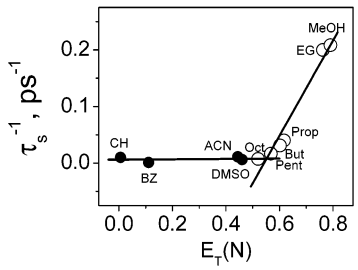

Figure 13. Plot of the decay rates (inverse of τ_3, which is given in Table 2) of the S_1(TICT) state as a function of E_T(N) values of the corresponding solvents.

4.8. Solvent Polarity and Hydrogen Bonding Effects on the Decay of the S_1 State. The property of the S_1(TICT) state of DMABP produced after completion of the conformational relaxation and solvation processes can be discussed in terms of the solvent polarity and hydrogen-bonding effect on the lifetime of the S_1 state. The lifetime, $\tau_3{}^b$(d), of the S_1(TICT) state in several solvents of varying polarity (dielectric constants varying in the range of 2−48) and hydrogen-bonding ability have been given in Table 2. The lifetime increases with decrease in polarity of the solvent. The decay rates (the inverse of $\tau_3{}^b$(d)) have been plotted as a function of $E_T(N)$ values of the solvents in Figure 13. The $E_T(N)$ values of the solvents, the most popular measure of the electronic solvation, are known to be as much a measure of hydrogen bonding to the solute as a measure of interaction with the solute dipoles.[76−79] In aprotic solvents, the lifetime of the S_1(TICT) state is nearly independent of $E_T(N)$. The steeper slope of the line representing the linear fit function in protic solvents indicates a strong hydrogen-bonding interaction between the S_1(TICT) state and the alcoholic solvents. The lifetime of the S_1(TICT) state becomes shorter in alcohols with stronger hydrogen bonding abilities or higher proticities. This fact possibly explains the weak emissive character of the S_1(TICT) state of DMABP in alcohols as compared to that in aprotic solvents.

4.9. Intersystem Crossing. In rigid matrixes at 77 K, in which the molecular motions are nearly frozen and both the conformational relaxation and solvation processes are considerably retarded, the main deactivation process of the S_1 state has been found to be the ISC process from the S_1(LE) state to the triplet state. The relative positions of the different triplet states on the PES diagram and the probable transitions for the ISC processes in different kinds of matrixes have been shown in Figure 11. Both in nonpolar and polar matrixes at 77 K, the ISC process takes place via the nonradiative transition from the S_1(LE) state, which is either a $\pi\pi^*$ state (in nonpolar solvents) or an ICT state (in polar solvents), to the $n\pi^*$ triplet state. This is an allowed transition, and hence, we observe very strong phosphorescence in all kinds of matrixes. However, since the $n\pi^*$ and $\pi\pi^*$ triplet states are energetically very close to each

other in nonpolar solvents, we observe dual phosphorescence in nonpolar solvents. However, in polar solvents, the $\pi\pi^*$ triplet state becomes energetically more stable than that of the $n\pi^*$ triplet state, and hence, the former becomes the lowest excited triplet state, which shows single-exponential phosphorescence decay.

The biexponential decay of the phosphorescence emission in MCH indicates the proximity of two kinds of triplet states, both of which are populated simultaneously. The shorter lifetime is associated with the $n\pi^*$ triplet state and the longer with the $\pi\pi^*$ triplet state. In methanol and acetonitrile, the energy difference between the two kinds of states becomes significant. In these matrixes, the energy of the $\pi\pi^*$ triplet state, which becomes the lowest energy triplet, is appreciably lowered as compared to that of the $n\pi^*$ triplet state, which is now the next higher energy triplet, i.e., T_2 ($n\pi^*$).

In nonpolar solvents at room temperature too, due to energetically favored positions of both the S_1(LE/$\pi\pi^*$) and S_1-(TICT) states with respect to that of the T_1($n\pi^*$) state, the intersystem crossing process remains very efficient. However, due to the partial $n\pi^*$ character of the T_1 state, the lifetime of the T_1 state in cyclohexane is very short (70 ns). In polar solvents at room temperature, the intersystem crossing process from the S_1(LE/ICT) to the energetically close T_1(ICT) state is a forbidden process and hence the triplet quantum yield is significantly small and could not be determined.

The dynamics of transient absorption monitored at 670 nm in butanol in the time-domain above 10 ps (inset of Figure 10) shows a small growth with the growth lifetime of 28 ps followed by a decay with the lifetime of about 60 ps. Comparing the growth lifetime of 28 ps with that of the S_1 state (τ_3^a(d) = 32 ps), which has been measured from the absorption decay at 900 nm, the transient spectrum recorded at 37 ps after the laser pulse (Figure 7B) could possibly be assigned to that of the triplet state. Hence, the triplet state of DMABP has a lifetime of about 60 ps in butanol.

5. Conclusions

We have studied the photophysics and the relaxation dynamics in the excited singlet and triplet states of DMABP in different classes of solvents. Large bathochromic shifts of the absorption spectra in more polar solvents suggest the ICT character of the LE state. Although DMABP is weakly fluorescent, it shows the features of "dual-fluorescence". Time-resolved measurements could reveal that conformational relaxation via diffusive twisting motion of the dimtheylaminophenyl group with respect to the benzoyl group is the main relaxation process in the S_1 state. Relaxation dynamics of DMABP has been explained using the three-state model, which involves the S_0 state and two adiabatically coupled S_1 states, the LE and TICT states. In aprotic solvents, a large Stokes shift between the absorption and fluorescence maxima at room temperature and absence of the main fluorescence band in rigid matrixes at 77 K suggest that the fluorescence emission mainly takes place from the S_1-(TICT) state. However, in alcoholic solvents, due to strong hydrogen-bonding interaction with the S_1(TICT) state, the latter is weakly fluorescent, and as a result, the fluorescence maximum arises due to emission from the S_1(LE) state. While in acetonitrile, a "fast-solvent", solvation and twisting processes may be happening simultaneously, whereas in all other solvents, the lifetime of the twisting process is much shorter than the average solvation time. However, by using the transient absorption technique, we could not obtain any direct evidence of the solvation process of the ICT state, which must be accompanying the twisting motion.

Acknowledgment. The authors gratefully acknowledge the help from Prof. Periasamy, TIFR, India in fluorescence lifetime measurements. Help from Dr. Chiranjib Majumder of Novel Material and Structural Chemistry Division, BARC, in the calculation of the ground state geometry of DMABP is gratefully acknowledged. The authors are also grateful to Drs. J. P. Mittal and T. Mukherjee for their constant encouragement.

References and Notes

(1) (a) Wagner, P. J. *Top. Curr. Chem.* **1976**, *66*. (b) Wagner, P. J.; Park, B. S. *Org. Photochem.* **1991**, *11*, 227.

(2) Scaiano, J. C. *J. Photochem.* **1973**, *2*, 81.

(3) Cohen, S. G.; Parola, A.; Parsons, G. H. *Chem. Rev.* **1973**, *73*, 141.

(4) Wagner, P. J.; Leavitt, R. A. *J. Am. Chem. Soc.* **1973**, *95*, 3669.

(5) Griller, D.; Howard, J. A.; Marriott, P. R.; Scaiano, J. C. *J. Am. Chem. Soc.* **1981**, *103*, 619.

(6) Wagner, P. J.; Truman, R. J.; Scaiano, J. C. *J. Am. Chem. Soc.* **1985**, *107*, 7093.

(7) Wagner, P. J.; Truman, R. J.; Puchalski, A. E.; Wake, R. *J. Am. Chem. Soc.* **1986**, *108*, 7727.

(8) Wagner, P. J. *Acc. Chem. Res.* **1971**, *4*, 5383.

(9) Wagner; P. J.; Thomas, M. J.; Harris, E. *J. Am. Chem. soc.* **1976**, *98*, 7675.

(10) Leigh, W. J.; Lathioor, E. C.; St. Pierre, M. J. *J. Am. Chem. Soc.* **1996**, *118*, 12339.

(11) Das, P. K.; Encinas, M. V.; Scaiano, J. C. *J. Am. Chem. Soc.* **1981**, *103*, 4154.

(12) Naguib, Y. M. A.; Steel, C.; Cohen, S. G. Young, M. A. *J. Phys. Chem.* **1987**, *91*, 3033.

(13) Bobrowski, K.; Marciniak, B.; Hug, G. L. *J. Am. Chem. Soc.* **1992**, *114*, 10279.

(14) (a) Peters, K. S.; Lee, J. *J. Phys. Chem.* **1993**, *97*, 3761. (b) Simon, J. D.; Peters, K. S. *J. Am. Chem. Soc.* **1981**, *103*, 6403. (c) Simon, J. D.; Peters, K. S. *J. Am. Chem. Soc.* **1982**, *104*, 6542. (d) Simon, J. D.; Peters, K. S. *J. Phys. Chem.* **1983**, *87*, 4855.

(15) Gramain, J. C.; Remuson, R. *J. Org. Chem.* **1985**, *50*, 1120.

(16) (a) Wagner, P. J.; Leavitt, R. A. *J. Am. Chem. Soc.* **1970**, *92*, 5806. (b) Wagner, P. J.; Lam, H. M.-H. *J. Am. Chem. Soc.* **1980**, *102*, 4167. (c) Wagner, P. J.; Puchalski, A. E. *J. Am. Chem. Soc.* **1978,** *100*, 5948. (d) Wagner, P. J.; Puchalski, A. E.; *J. Am. Chem. Soc.* **1980**, *102*, 6177. (e) Wagner, P. J.; Kemppainen, A. E.; Schott, H. N. *J. Am. Chem. Soc.* **1973**, *95*, 5604. (f) Wagner, P. J.; Siebert, E. J. *J. Am. Chem. Soc.* **1981**, *103*, 7329.

(17) Wan, J. K. S.; McCormick, R. N.; Baum, E. J.; Pitts, J. N. *J. Am. Chem. Soc.* **1965**, *87*, 4409.

(18) Kavarnos, G. J.; Turro, N. J. *Chem. Rev.* **1986**, *86*, 401.

(19) (a) Cohen, S. G.; Parola, A.; Parsons, G. H. *Chem. Rev.* **1973**, *73*, 141.3. (b) Cohen, S. G.; Stein, N.; Chao, H. M. *J. Am. Chem. Soc.* **1968**, *90*, 521. (c) Cohen, S. G.; Chao, H. C. *J. Am. Chem. Soc.* **1968**, *90*, 165.

(20) Wagner, P. J.; Truman, R. J.; Puchalski, A. E.; Wake, R. *J. Am. Chem. Soc.* **1986**, *108*, 7727.

(21) (a) Wagner, P. J.; Kemppainen, A. E.; Schott, H. N. *J. Am. Chem. Soc.* **1973**, *95*, 5604. (b) Wagner, P. J.; Siebert, E. J. *J. Am. Chem. Soc.* **1981**, *103*, 7329. (c) Wagner, P. J. *Acc. Chem. Res.* **1971**, *4*, 168. (d) Wagner, P. J. *J. Am. Chem. Soc.* **1967**, *89*, 5898. (e) Wagner, P. J.; May, M. J.; Haug, A.; Graber, D. R. *J. Am. Chem. Soc.* **1970**, *92*, 5269. (f) Wagner, P. J.; Kemppainen, A. E. *J. Am. Chem. Soc.* **1968**, *90*, 5898. (g) Wagner, P. J.; Kemppainen, A. E.; Schott, H. N. *J. Am. Chem. Soc.* **1970**, *92*, 5280. (h) Wagner, P. J.; Schott, H. N. *J. Am. Chem. Soc.* **1969**, *91*, 5383.

(22) Berger, M.; McAlpine, E.; Steel, C. *J. Am. Chem. Soc.* **1978,** *100*, 5147.

(23) Wolf, W. M.; Brown, R. E.; Singer, L. A. *J. Am. Chem. Soc.* **1977**, *99*, 526.

(24) (a) Yang, N. C.; Dusenbery, R. L. *Mol. Photochem.* **1969**, *1*, 159. (b) Dym, S.; Hochstrasser, R. M. *J. Chem. Phys.* **1969**, 51, 2458. (c) Lutz, H.; Duval, M. C.; Breheret, E.; Lindqvist, L. *J. Phys. Chem.* **1972**, *76*, 821. (d) Jovanovic, S. V.; Morris, D. G.; Pliva, C. N.; Scaiano, J. C. *J. Photochem. Photobiol. A: Chem.* **1997**, *107*, 153. (e) Cohen, S. G.; Davis, G. A.; Clark, W. D. K. *J. Am. Chem. Soc.* **1972**, *94*, 869.

(25) Kearns, D. R.; Case, W. A. *J. Am. Chem. Soc.* **1966**, *88*, 5087.

(26) (a) Porter, G.; Suppan, P. *Trans. Faraday Soc.* **1966**, *62*, 3375. (b) Porter, G.; Suppan, P. *Trans. Faraday Soc.* **1965**, *61*, 1664. (c) Beckett, A.; Porter, G. *Trans. Faraday Soc.* **1963**, *59*, 2038.

(27) Bhasikuttan, A. C.; Singh, A. K.; D. K. Palit, Sapre, A. V. Mittal, J. P. *J. Phys. Chem. A* **1998**, *102*, 3470.

(28) Aspari, P.; Ghoneim, N; Haselbach, E.; Von Raumer, M.; Suppan, P.; Vauthey, E. *J. Chem. Soc., Faraday Trans.* **1996**, *92*, 1689.

(29) Ghoneim, N.; Monbelli, A.; Pilloud, D.; Suppan, P. *J. Photochem. Photobiol. A: Chem.* **1996**, *94*, 145.
(30) Singh, A. K.; Bhasikuttan, A. C.; Palit, D. K.; Mittal, J. P. *J. Phys. Chem. A* **2000**, *104*, 7002
(31) Singh, A. K.; Palit, D. K.; Mittal, J. P. *Res. Chem. Intermed*. **2001**, *27*, 125.
(32) Veldhoven, E. von,; Zhang, H.; Rettig, W.; Brown, R. G.; Hepworth, J. D.; Glasbeek, M. *Chem. Phys. Lett*. **2002**, *363*, 189.
(33) Shoute, L. C. T. *Chem. Phys. Lett*. **1992,** *195*, 255.
(34) Prater, K.; Freund, W. L.; Bowman, R. M. *Chem. Phys. Lett*. **1998**, *295*, 82.
(35) Grabowski, Z. R.; Rotkiewicz, K.; Rettig, W. Chem. Rev. **2003**, *103*, 3857.
(36) (a) Meyer, M.; Mialocq, J.-C. *Opt. Commun*. **1987**, *64*, 264. (b). Rettig, W.; Majenz, W. *Chem. Phys. Lett.* **1993**, *201*, 153. (c). Meyer, M.; Mialocq, J.-C.; Perly, B. *J. Phys. Chem.* **1990**, *94*, 98.
(37) Martin, M. M.; Plaza, P.; Changenet, P.; Meyer, Y. H. *J. Photochem. Photobiol. A: Chem.* **1997**, *105*, 197.
(38) Duxbury, D. F. *Chem. Rev.* **1993**, *93*, 381.
(39) Nagasawa, Y.; Ando, Y.; Kataoka, D.; Matsuka, H.; Miyasaka, H.; Okada, T. *J. Phys. Chem. A* **2002**, *106*, 2024.
(40) Mokhtari, A.; Fini, L.; Chesnoy, J. *J. Chem. Phys*. **1987**, *87*, 3429.
(41) (a) van der Meer, M. J.; Zhang, H.; Glasbeek, M. *J. Chem. Phys.* **2000**, *112*, 2878. (b) Changenet, P.; Zhang, H.; van der Meer, M. J.; Glasbeek, M.; Plaza, P.; Martin, M. *J. Phys. Chem. A* **1998**, *102*, 6716.
(42) Vogel, M.; Rettig, W.; Sens, R.; Drexhage, K. H. *Chem. Phys. Lett*. **1988**, *147*, 452.
(43) (a) Grabowski, Z. R.; Rotkiewicz, K.; Rubaszewka, W.; Kirkor-Kaminska, E. *Acta Phys. Pol. A* **1978**, *54*, 767. (b) Grabowski, Z. R.; Dobkowski, J. *Pure Appl. Chem*. **1983**, *55*, 245.
(44) (a) Vogel, M.; Rettig, W.; Heimbach, P. *J. Photochem. Photobiol. A: Chem*. **1991**, *61*, 65. (b) Hara, K.; Kometani, N.; Kajimoto, O. *J. Phys. Chem*. **1996**, *100*, 1488.
(45) (a) Rettig, W.; Majenz, W.; Lapouyade, R.; Hancke, G. *J. Photochem. Photobiol. A: Chem.* **1992**, *62*, 415. (b) Letard, J. F.; Lapouyade, R.; Rettig, *J. Am. Chem. Soc*. **1993**, *115*, 2441. (c) Lapouyade, R.; Kuhn, A.; Letard, J. F.; Rettig, W. *Chem. Phys. Lett.* **1993**, *208*, 48.
(46) Morimoto, A.; Biczok, L.; Yatsuhasi, T.; Shimada, T.; Baba, S.; Tachibana, H.; Tryk, D. A.; Inoue, H. *J. Phys. Chem. A* **2002**, *106*, 10089.
(47) (a) Gulbinas, V.; Markovitsi, D.; Gustavsson, T.; Karpicz, R.; Veber, M. *J. Phys. Chem. A* **2000**, *104*, 5181. (b) Abramavicius, D.; Gulbinas, V.; Hayashi, M.; Lin, S. H. *J. Phys. Chem. A* **2002**, *106*, 8864.
(48) Gulnibas, V.; Kodis, G.; Jursenas, S.; Valkunas, L.; Gruodis, A.; Mialocq, J.-C.; Pommeret, S.; Gustavsson, T. *J. Phys. Chem. A* **1999**, *103*, 3969.
(49) Periasamy, N.; Doraiswamy, S.; Maiya, G. B.; Venkataraman, B. *J. Chem. Phys.* **1988**, 88, 681.
(50) Bakshi, M. S. *J. Chem. Soc., Faraday Trans*. **1993**, 89, 3049.
(51) (a) Lippert, E. *Z. Naturforsch.* **1955**, *10a*, 541. (b) Mataga, N.; Kaifu, Y.; Koizumi, M. *Bull. Chem. Soc. Jpn.* **1995**, *28*, 690.
(52) Edward, J. T., *J. Chem. ed.* **1970**, 47, 261.
(53) Riddik, J. A.; Bunger, W. B.; Sakano, T. K. *Organic Solvents*; Wiley: New York, 1986.
(54) Horng, M. L.; Gardecki, J. A.; Papazyan, A.; Maroncelli, M. *J. Phys. Chem.* **1995**, *99*, 2502
(55) (a) Palit, D. K.; Pal, H.; Mukherjee, T.; Mittal, J. P. *J. Chem. Soc., Faraday Trans*. **1990**, *86*, 3861. (b) Folm, S. R.; Barbara, P. F. *J. Phys. Chem*. **1985**, *89*, 4489. (c) Barbara, P. F.; Walsh, P. K.; Brus, L. E. *J. Phys. Chem*. **1989**, *93*, 29. (d) Avouris, P.; Gilbert, W. M.; El-Sayed, M. A. *Chem. Rev*. **1997**, *77*, 793. (e) Smulevich, G.; Foggi, P.; Feis, A.; Marzocchi, M. P. *J. Chem. Phys*. **1987**, *87*, 5664.
(56) (a) Yatsuhashi, T.; Nakajima, Y.; Shimada, T.; Inoue, H. *J. Phys. Chem. A* **1998,** *102*, 3018, 8657. (b) Biezok, L.; Yatsuhashi, T.; Be'rces, T.; Inoue, H.; *Phys. Chem. Chem. Phys.* **2001**, *3*, 980.
(57) *Conformational Analysis of Molecules in Excited states*; Waluk, J., Ed.; Wiley: New York, 2000.
(58) Rettig, W.; Maus, M. In *Conformational Analysis of Molecules in Excited states*; Waluk, J. Ed.; Wiley: New York, 2000; p 1.
(59) Rettig, W. *Top. Curr. Chem.* **1994**, *169*, 253.
(60) (a) Du, M.; Fleming, G. R.; *Biophys. Chem.* **1993**, *48*, 101. (b) Chosrowjan, H.; Mataga, N.; Nakashima, N.; Imamaoto, Y.; Tokunaga, F. *Chem. Phys. Lett.* **1997**, *270*, 267.
(61) (a) Palit, D. K.; Singh, A. K.; Bhasikuttan, A. C.; Mittal, J. P. *J. Phys. Chem. A* **2001,** *105*, 6294. (b) Sanchez-Galvez, A.; Hunt, P.; Robb, M. A.; Olivucci, M.; Vreven, T.; Schelgel, H. B. *J. Am. Chem. Soc*. **2000**, *122*, 291.
(62) Kramers, H. A. *Physica* **1940**, *1*, 284.
(63) Fleming, G. R. *Chemical Applications of Ultrafast Spectroscopy*; Oxford University Press: New York, 1986; p 186.
(64) Waldeck, W. H. *Chem. Rev.* **1991**, *91*, 415.
(65) Nikowa, L.; Schwarzer, D.; Troe, J.; Schroeder, J. *J. Chem. Phys.* **1992**, *97*, 4827.
(66) Rodier, J.-M.; Myers, A. B. *J. Am. Chem. Soc*. **1993**, *115*, 1079.
(67) Rosenthal, S. J.; Xie, X. L.; Du, M.; Fleming, G. R. *J. Chem. Phys.* **1991**, *95*, 4715.
(68) Rosenthal, S. J.; Jimenez, R.; Fleming, G. R.; Kumar, P. V.; Maroncelli, M. *J. Mol. Liq.* **1994**, *60*, 25.
(69) Jimenez, R.; Fleming, G. R.; Kumar, P. V.; Maroncelli, M. *Nature*, **1994**, *369*, 471.
(70) Joo, T.; Jia, Y.; Yu, J.-Y.; Lang, M.; Fleming, G. R.; *J. Chem. Phys.* **1996**, *104*, 6089.
(71) Maroncelli, M. *J. Mol. Liq.* **1993**, *57*, 1.
(72) Polimeno, A.; Barbon, A.; Nordio, P. L.; Rettig, W. *J. Phys. Chem*. **1994**, *98*, 12158.
(73) Giacometti, G.; Moro, G. J.; Nordio. P. L.; Polimeno, A. *J. Mol. Liq*. **1989**, *42*, 19.
(74) Fonseca, T.; Kim, H. J.; Hynes, J. T. *J. Mol. Liq*. **1994**, *60*, 161.
(75) Dorairaj, S.; Kim, H. *J. Phys. Chem. A* **2002**, *101*, 2322
(76) Marcus, Y. *J. Solution Chem*. **1991**, *20*, 929.
(77) Reichardt, C. *Solvents and Solvent Effects in Organic Chemistry*; VCH: New York, 1990.
(78) Fowler, F. W.; Katritezky, A. R.; Rutherford, R. J. D. *J. Chem. Soc. B* **1971**, *3*, 460.
(79) Reid, P. J.; Alex, S.; Jarzeba, W.; Schlief, R. E.; Johnson, A. E.; Barbara, P. F. *Chem. Phys. Lett*. **1994**, *229*, 93.